Australian Government | ANSTO

Scattering Part II

AOFSRR School @ Australian Synchrotron

13/08/2024

Andrew J. Clulow

Senior Beamline Scientist - BioSAXS

Email: as-biosaxs@ansto.gov.au

Science. Ingenuity. Sustainability.

Breakdown

- **The Scattering Beamlines**
  - SAXS/WAXS and BioSAXS – key differences
- **Data Reduction & Content**
- **Science Examples**

ANSTO

Scattering Beamlines

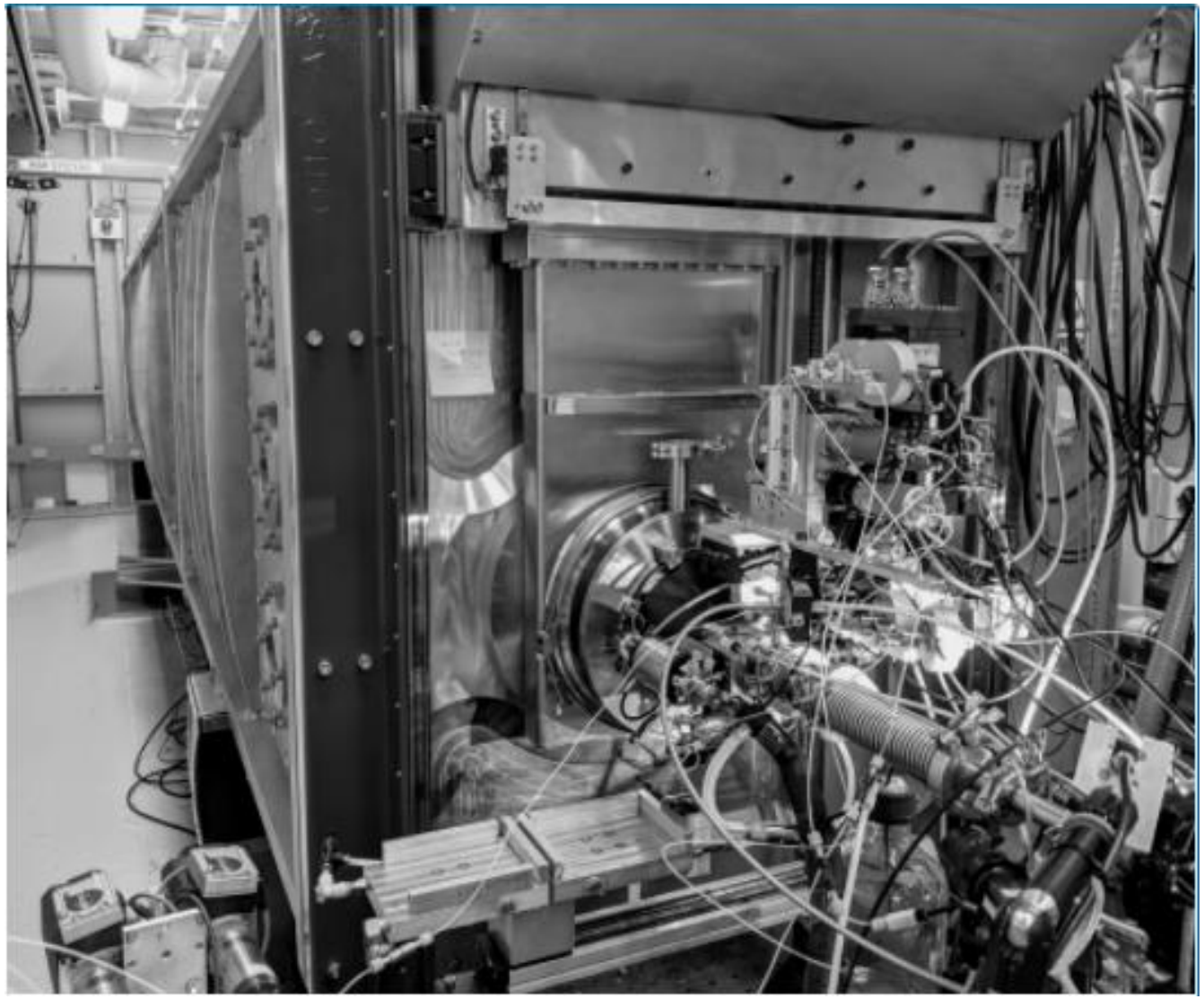

Small and Wide Angle
X-ray scattering
(SAXS/WAXS)

Biological Small Angle
X-ray Scattering
(BioSAXS)

ANSTO

Generic Beamline Layout

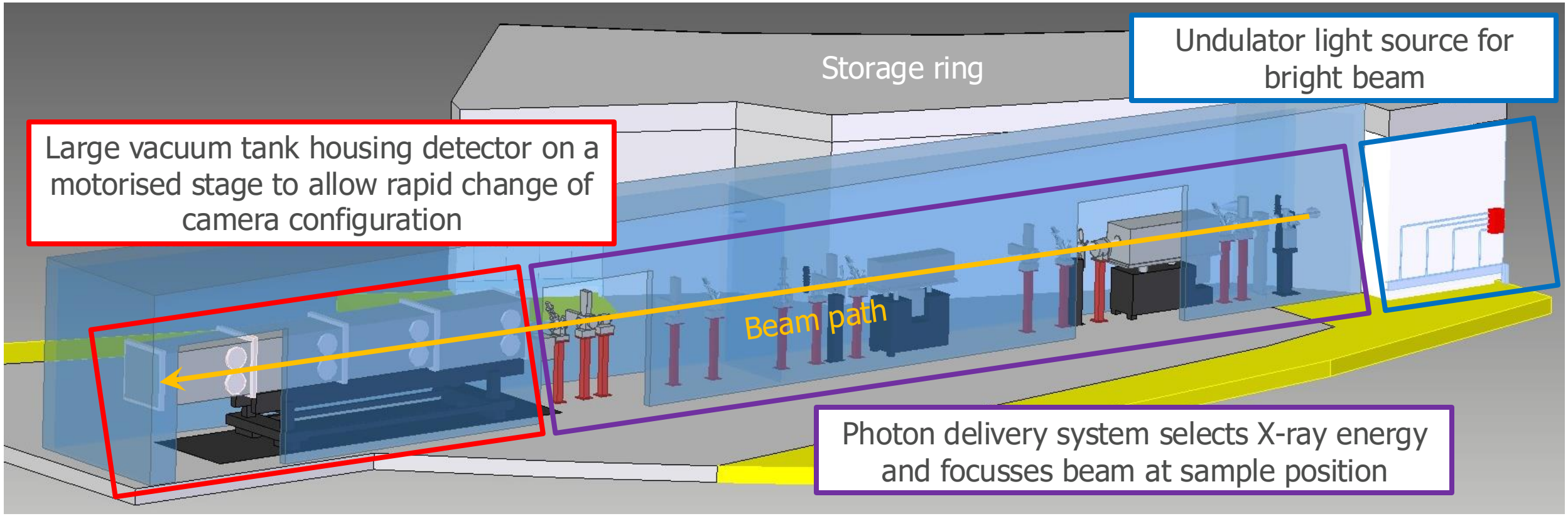

In general, SAXS beamlines have

1) Well-defined incident beam
2) High flux at sample 10^{12}-10^{14} photons s^{-1}
3) Offer a range of photon energies (X-ray wavelengths)
4) Range of scattering angles by moving detector closer to/further from the sample

ANSTO

SAXS Beamlines at the Aus. Synchrotron

Small and Wide Angle X-ray scattering (SAXS/WAXS)

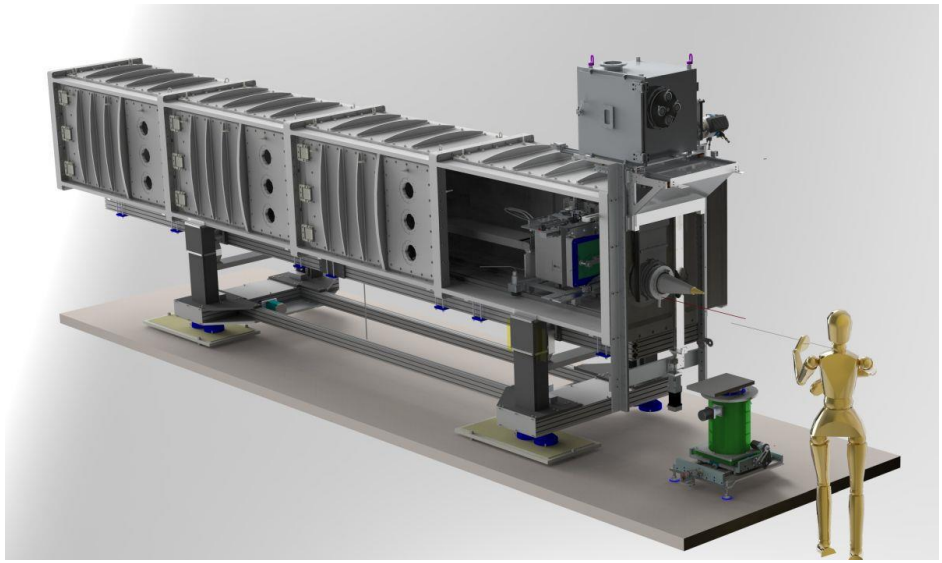

Takes all samples types (solid, liquid gel)

Small beam spot with microfocus capability

Flux = 10^{12}-10^{13} photons/s

Energy range = 5-20 keV

Samples in vacuum and in air

BioSAXS

Optimised for solution scattering (liquids)

Larger beam spot

Flux = 10^{13}-10^{14} photons/s

Energy range = 8-15 keV (usually 12.4 keV)

Coflow

ANSTO

Data Reduction and Content

ANSTO

Typical Small Angle Scattering Experiment

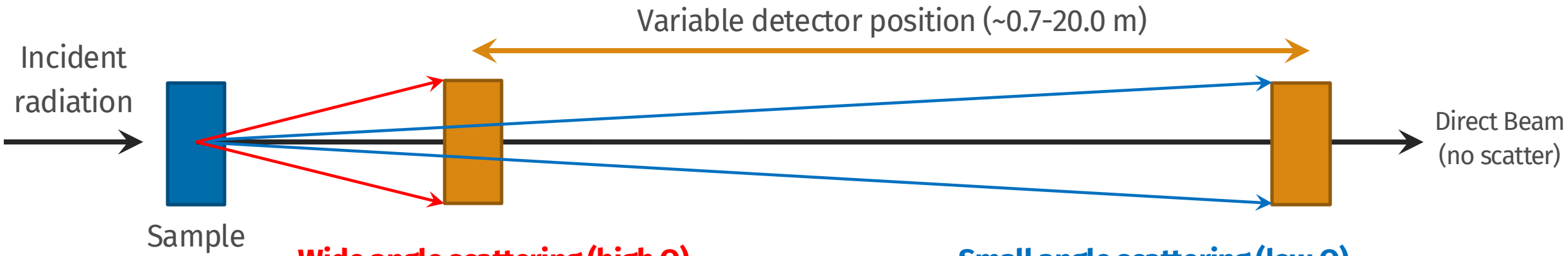

Wide angle scattering (high Q)

Å-nm structuring

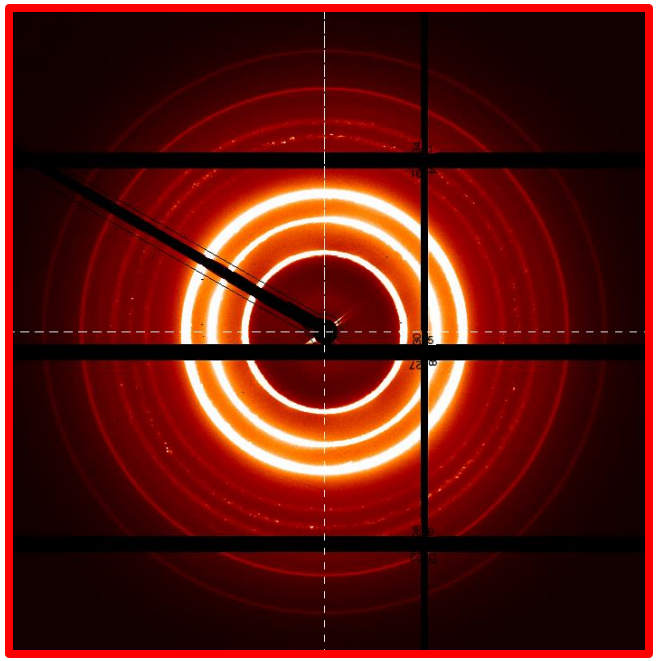

Crystals (diffraction)

Liquid crystals

Small micelles/particles

Small angle scattering (low Q)

nm-µm structuring

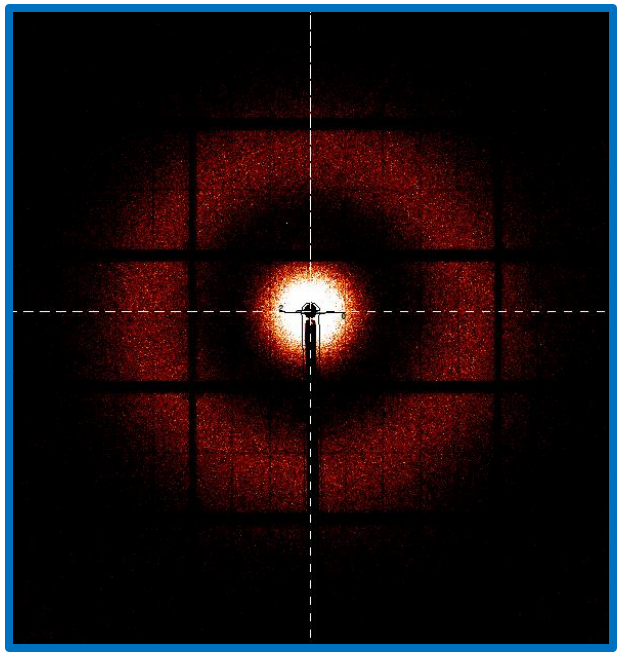

Aggregate structures

Larger micelles

Vesicles

Macromolecules

Proteins

ANSTO

Data Reduction

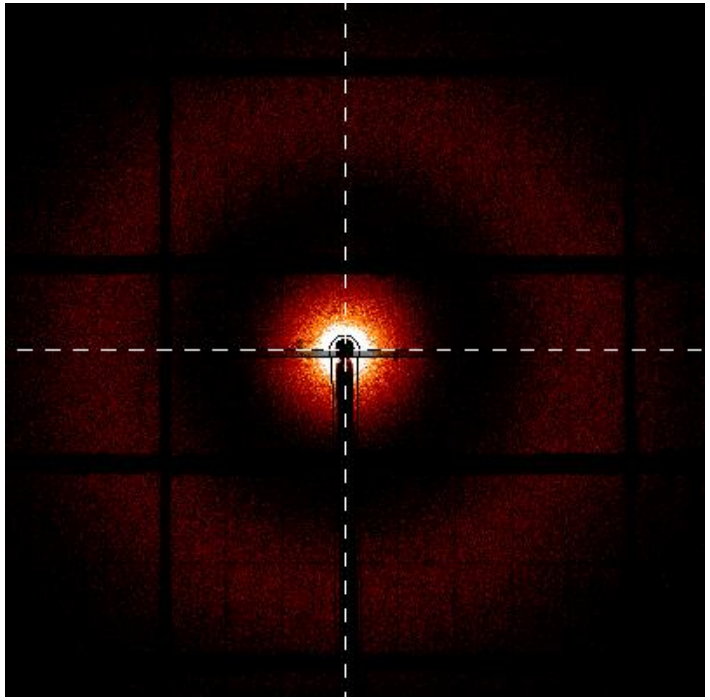

Raw 2D detector image with
Beamstop shadow
Beam centre crosshairs
Gaps between detector plates

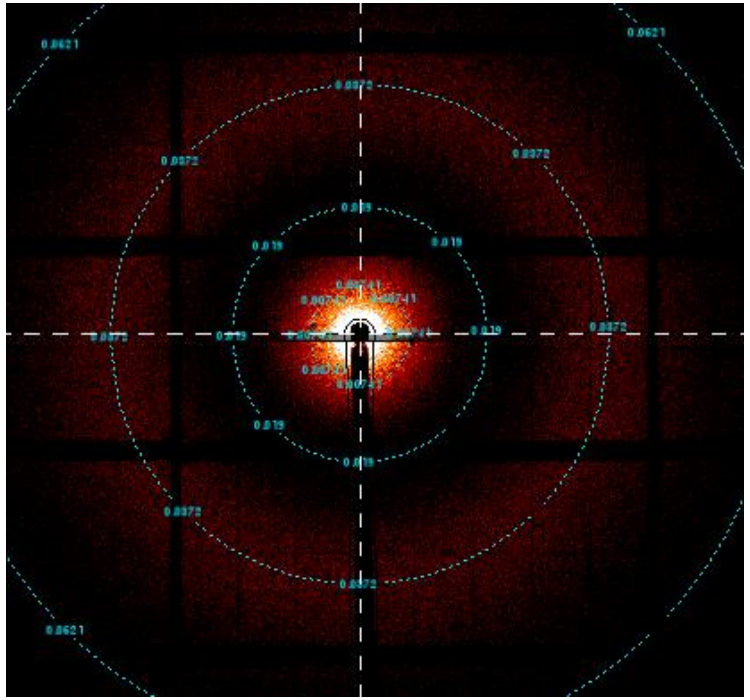

We calibrate the scattering angle/*q* vector at each point on the detector with a standard sample

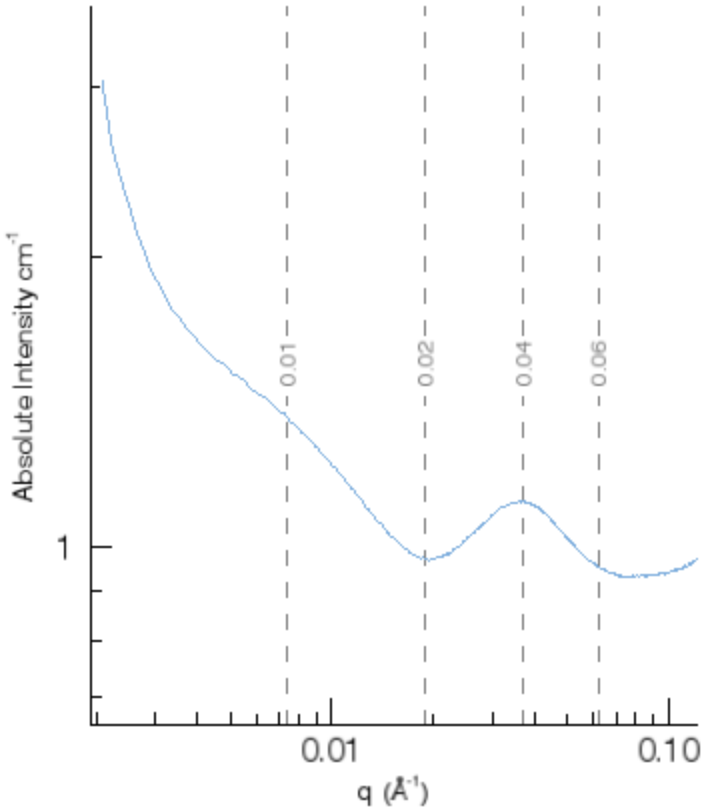

Software integrates the scattered X-ray intensity along each of the rings to generate an *I* vs *q* plot

ANSTO

Two Measurements Required

TOTAL Scattering

(sample + matrix/dispersant + instrument background)

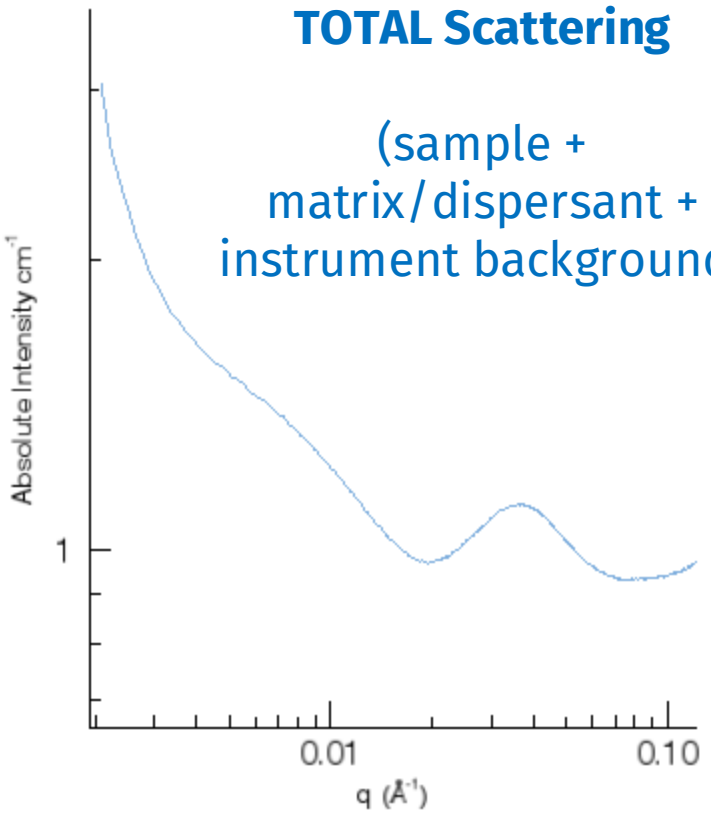

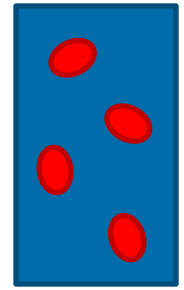

MATRIX (Background) Scattering

(matrix/dispersant + instrument background)

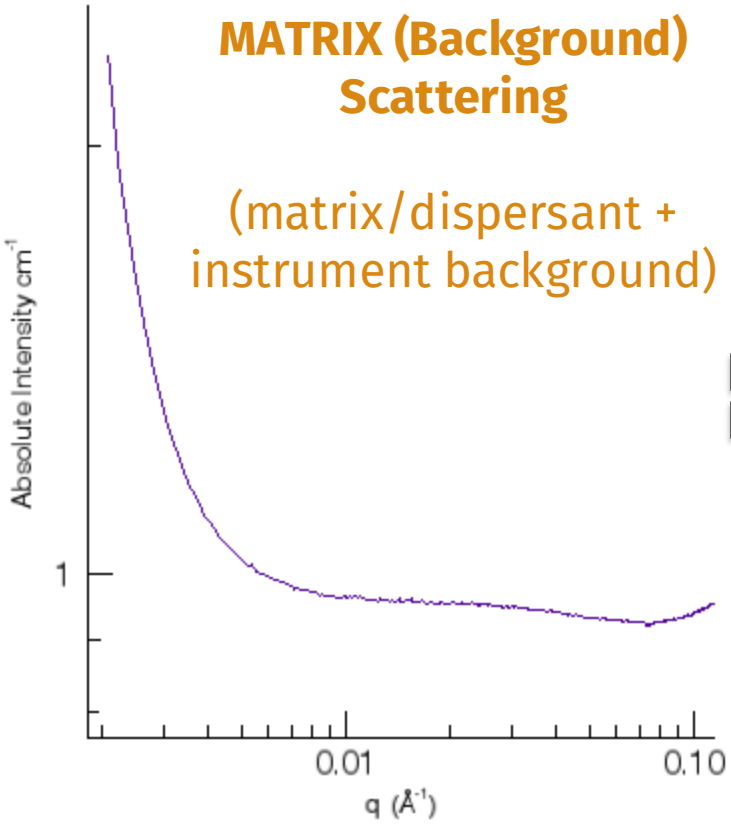

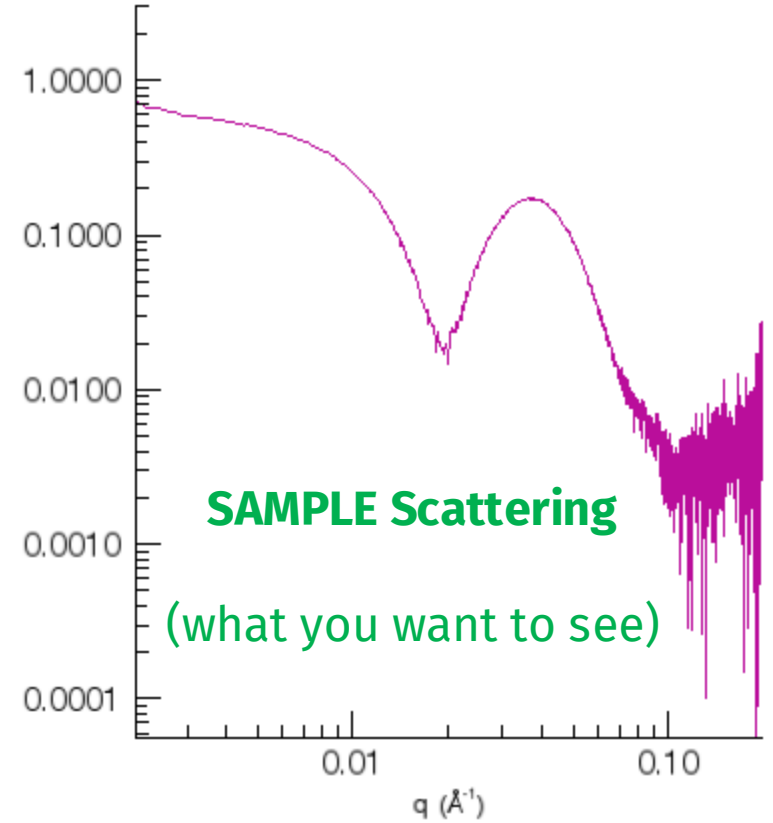

SAMPLE Scattering

(what you want to see)

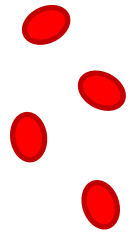

What Does Reduced Data Look Like?

Background subtraction

Scaling

Stitching

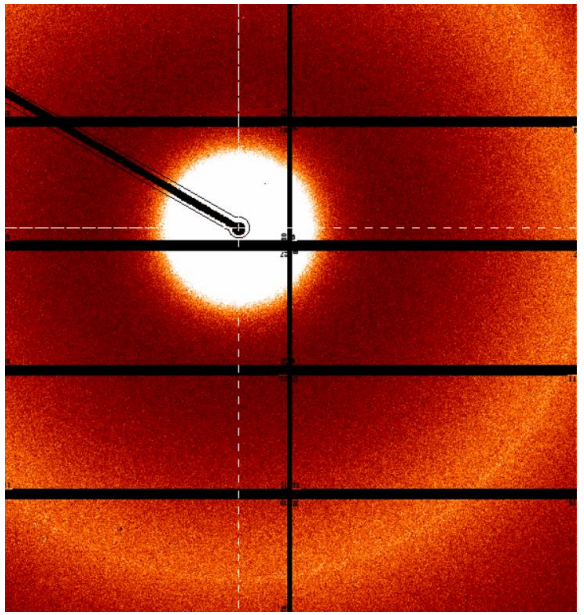

Data from a sample 7 m from the detector

radial integration

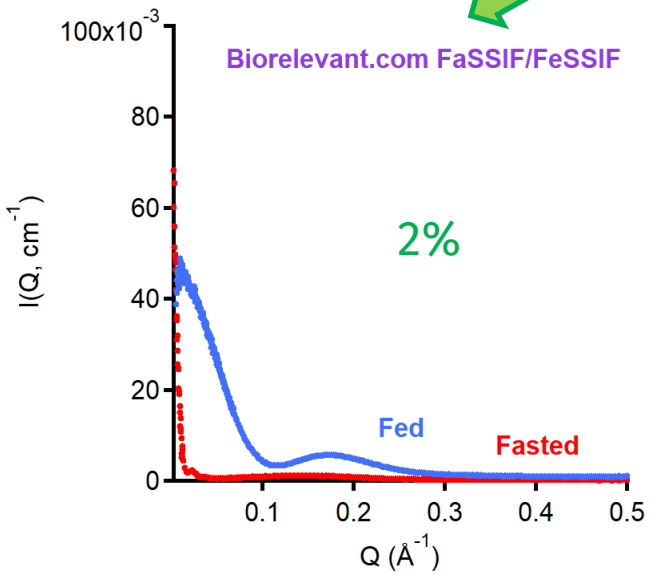

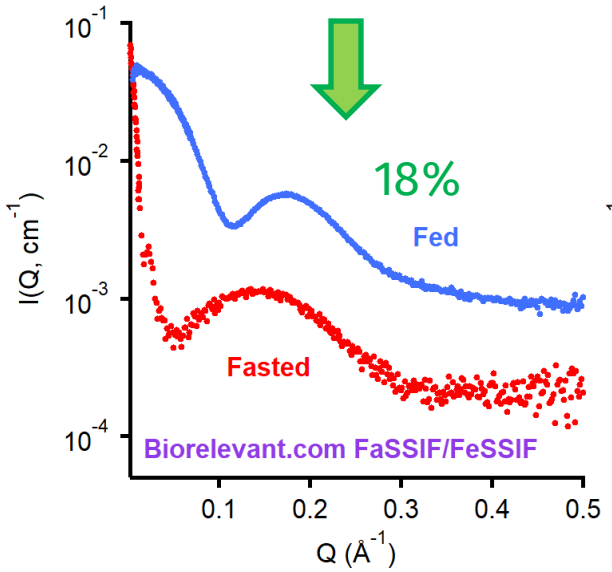

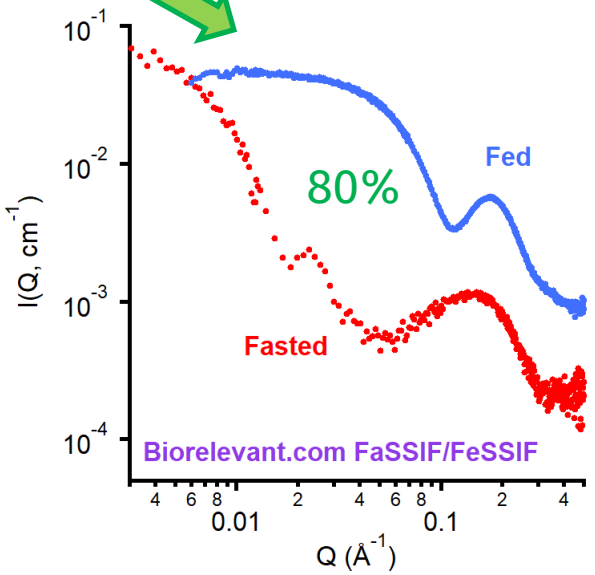

Low-hanging Fruit (Qualitative Information up for Grabs)

ANSTO

Typical Data Content – Particle Structure

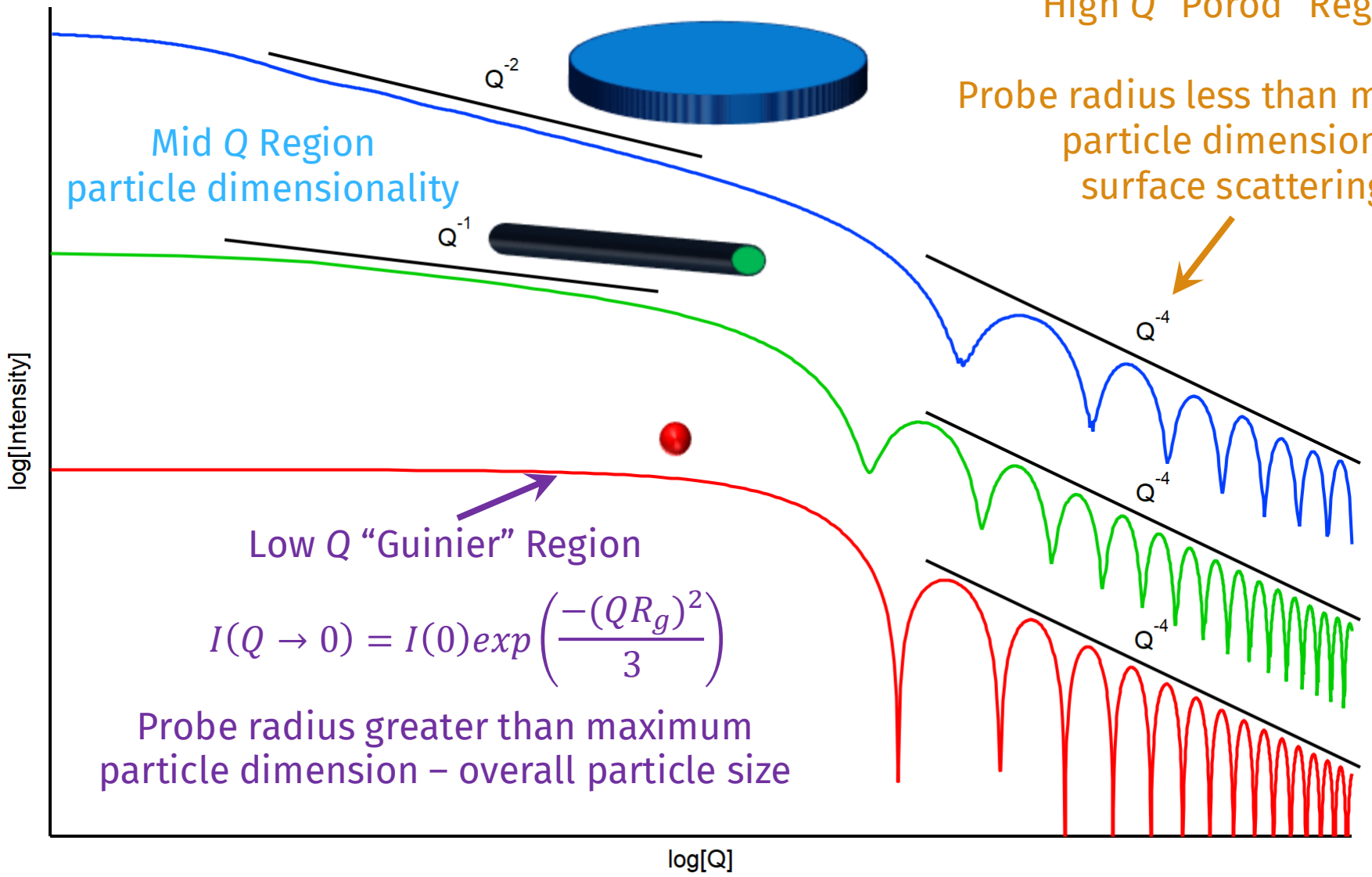

Particle size

Particle shape

Surface roughness

(simulated data for ideal particle shapes)

ANSTO

Typical Data Content – Guinier Fitting

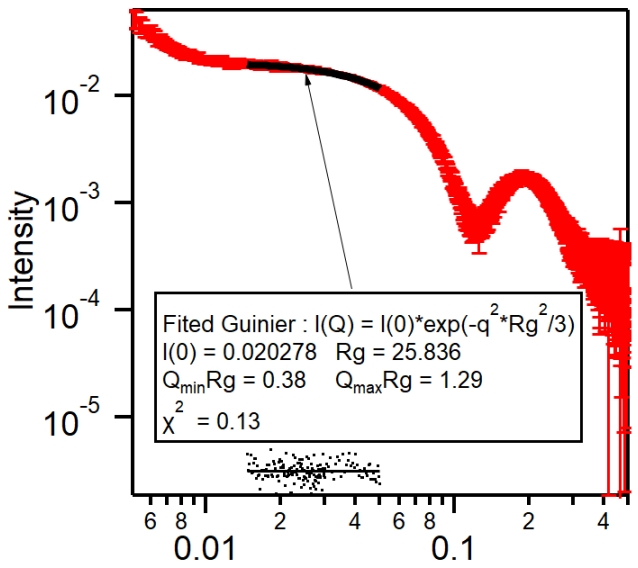

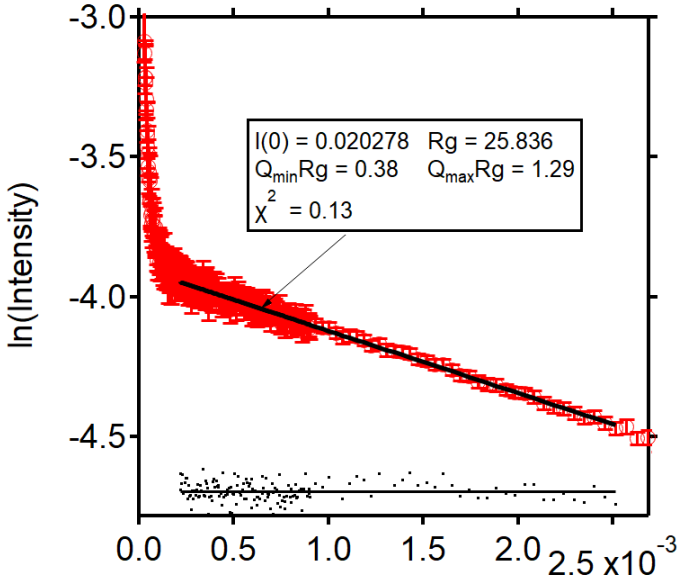

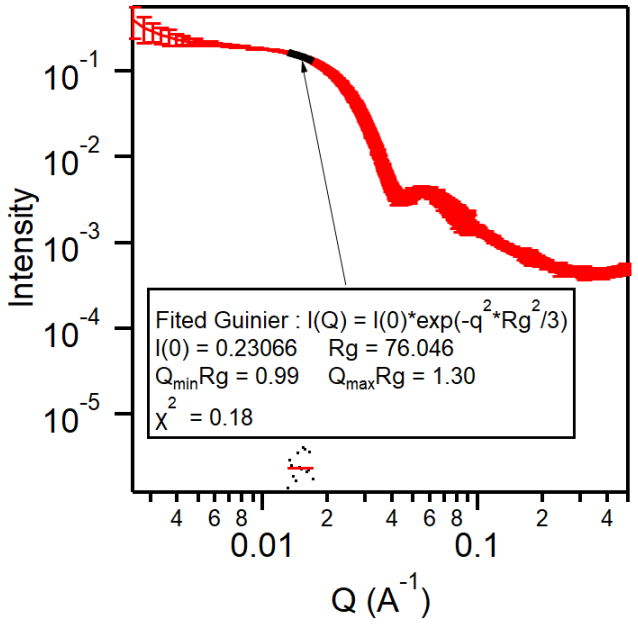

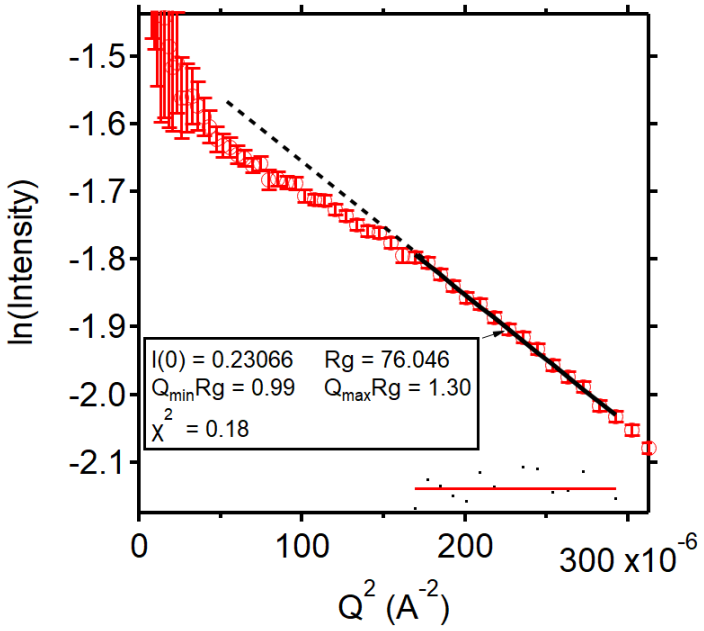

Affords the radius of gyration (R_g) of the electron density in the particle (SLD for neutrons)

Gives a measure of overall particle size

Only valid at low q ($qR_g < 1.3$ for spherical particles)

Can provide a measure of aggregation/interparticle interactions (structure factor)

***Data processing/visualisation in IRENA macros (IgorPro)**

ANSTO

Typical Data Content – Kratky Plot

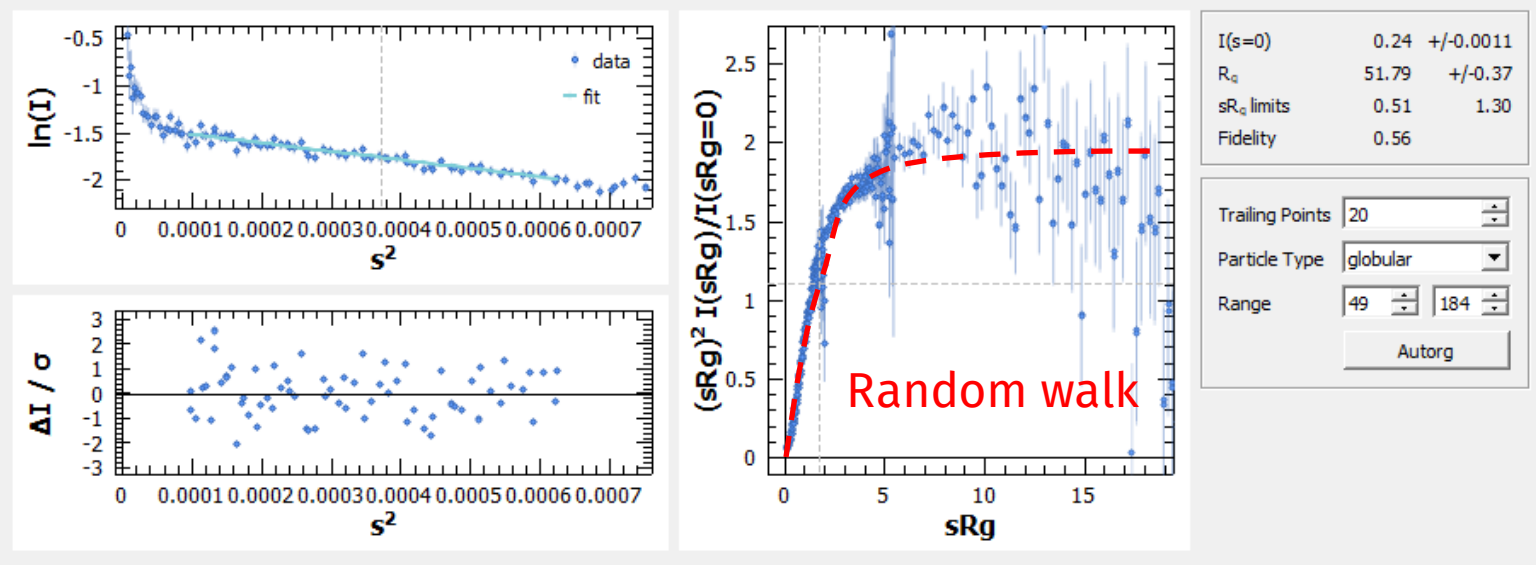

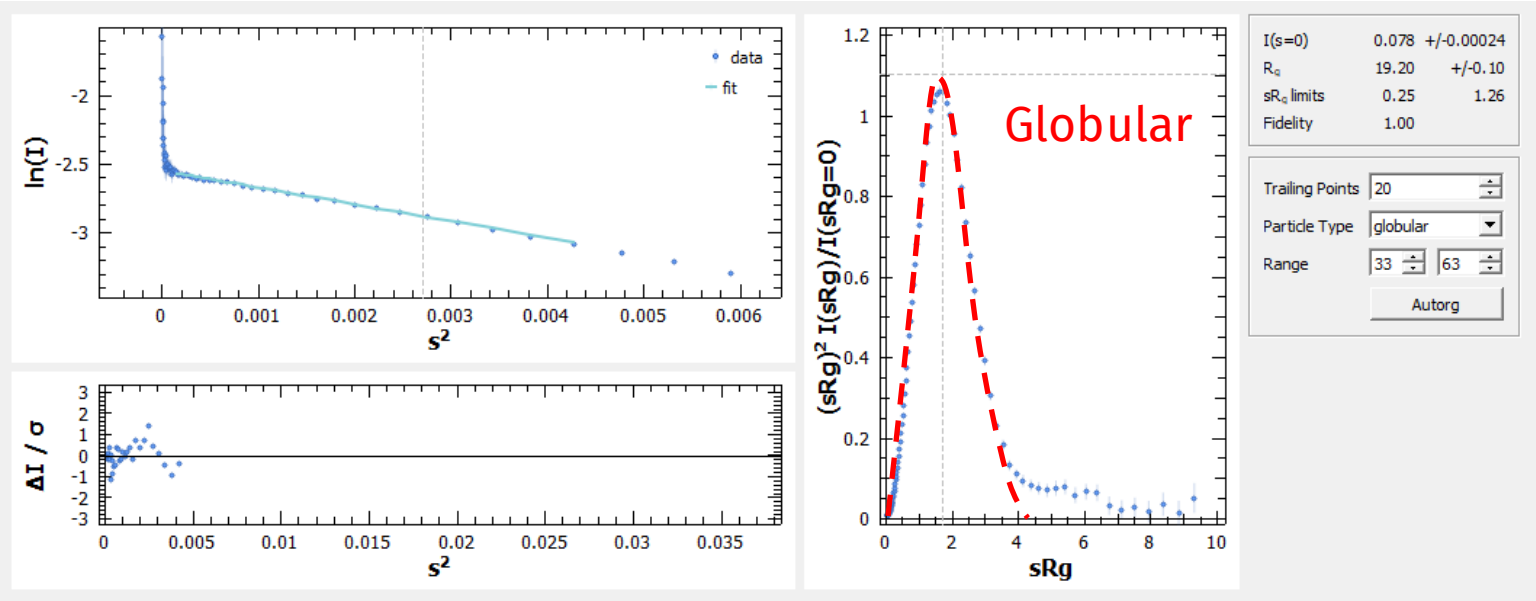

Plot of Iq^2 versus q

Gives a rough indication of the level of ordering in the particle

A high qR_g plateau is indicative of a random walk structure – theta polymer/disordered protein sections

A peak in dimensionless Kratky plot around $I(qR_g)^2/I(0) = 1.1$, $qR_g = \sqrt{3}$ indicates globular particle

*Data processing/visualisation in ATSAS (uses s not q)

ANSTO

Time-resolved SAXS (Stopped Flow)

Protein and nucleic acid folding and unfolding

Structural changes of organic and inorganic compounds

Ligand binding conformational changes

Aiming for temporal resolution on the order of 3 ms on BioSAXS

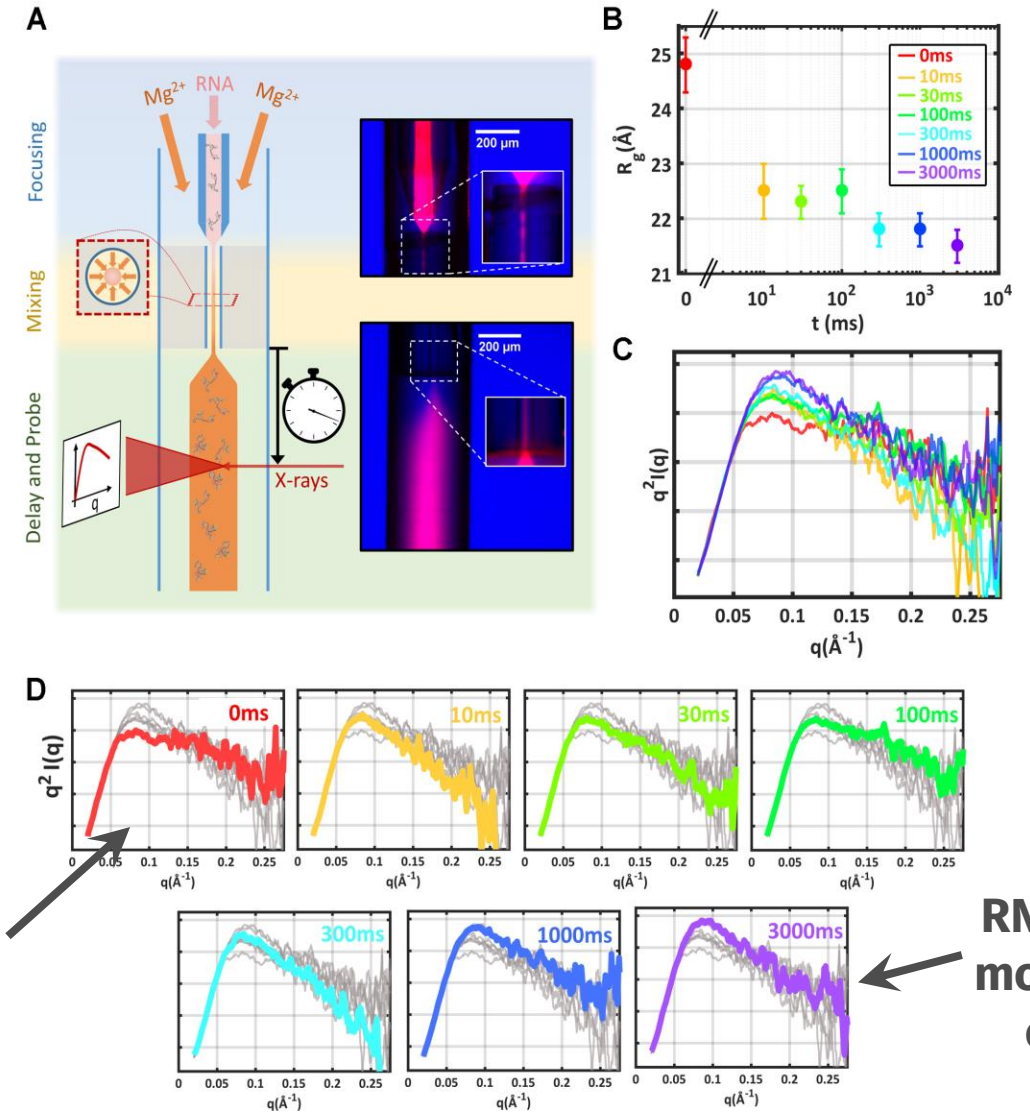

Initially relatively unstructured RNA

RNA becomes more globular over time

Plumridge *et al. Nucleic Acids Res.* 2018, 46 (14), 7354-7365

ANSTO

Protein Scattering

ANSTO

Typical Data Content – Protein Structure

Rigid body/bead ab initio modelling

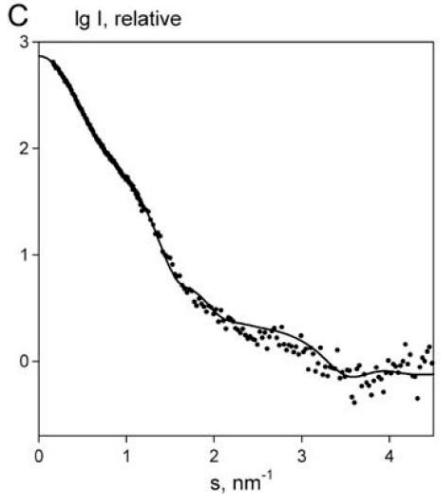

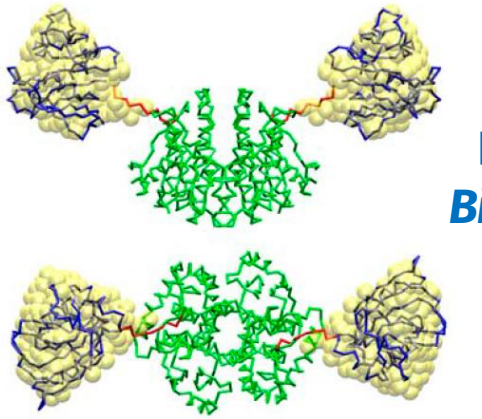

Petoukhov *et al.* *Biophys J.* 2005, 89, 1237-1250

SEC-SAXS

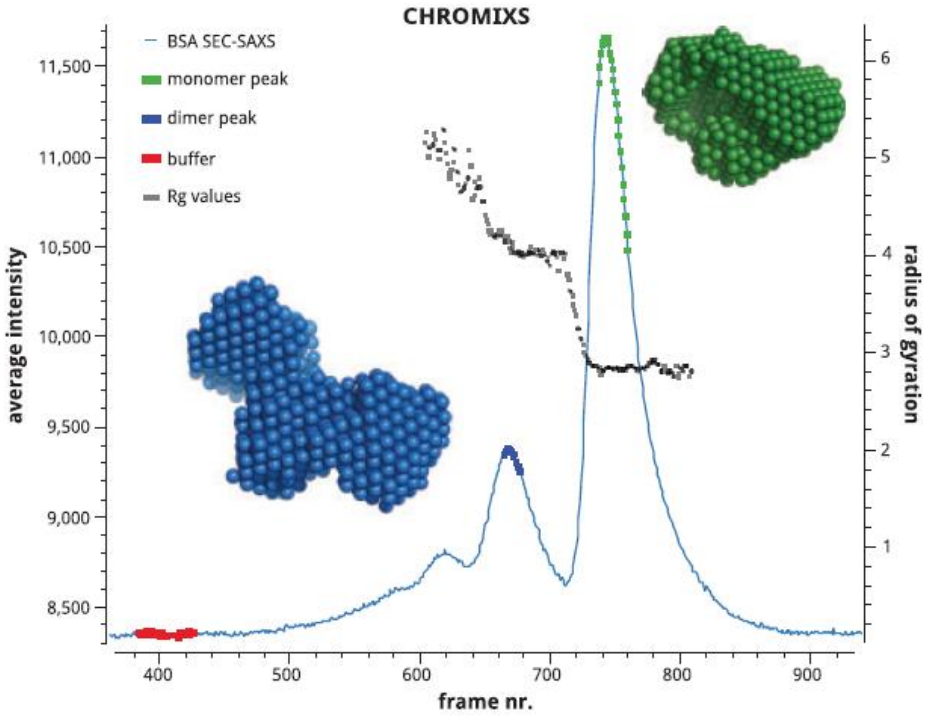

Panjkovich *et al. Bioinformatics* 2018, 34 (11), 1944-1946

Intermediates and oligomers in evolving mixtures

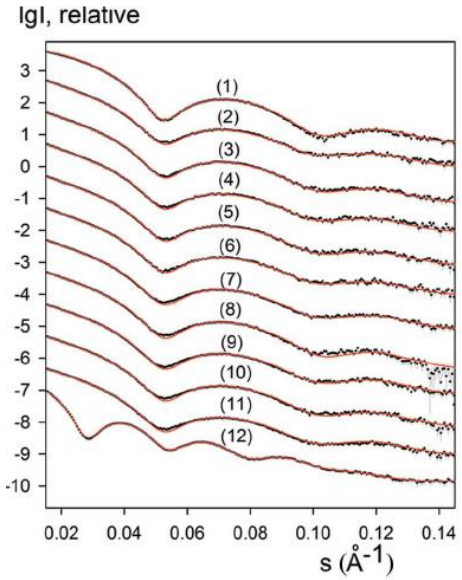

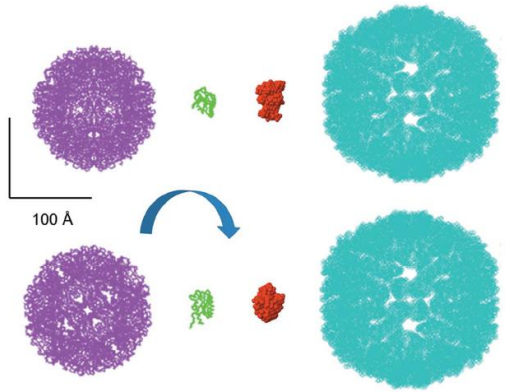

Konarev *et al. IUCrJ* 2018, 5, 402-409

ATSAS 3.0 Overview

Manalastas-Cantos *et al. J. Appl. Crystallogr.* 2021, 54, 343-355

ANSTO

Comparing Solution and Crystal Structures

E. coli O157:H7 phage FAHEc1 endolysin, LysF1
(T4 Lysozyme-like endolysin)

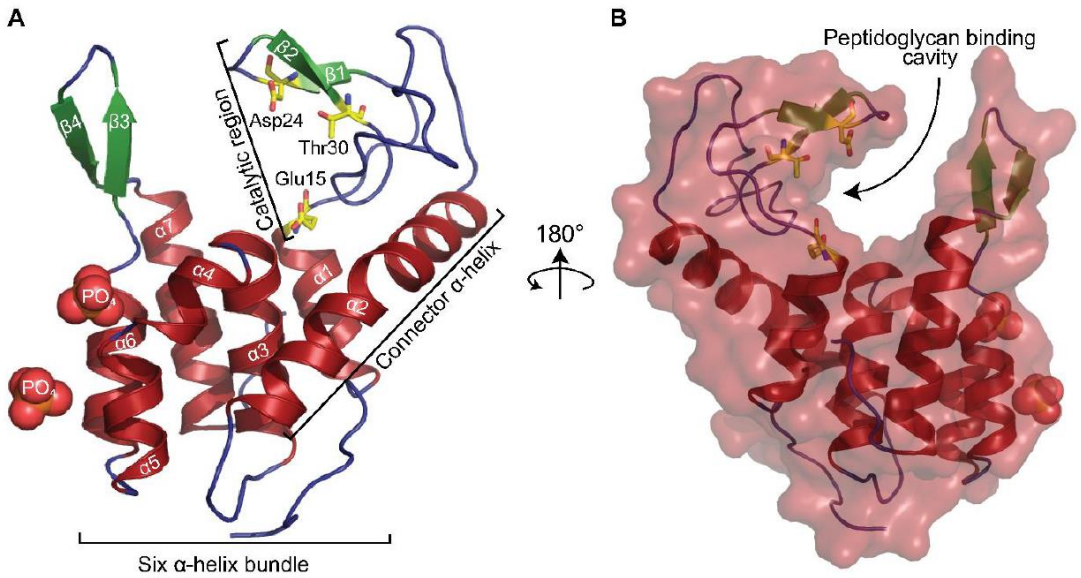

Specific enzymes for the breakdown of bacterial cell walls (phage therapy)

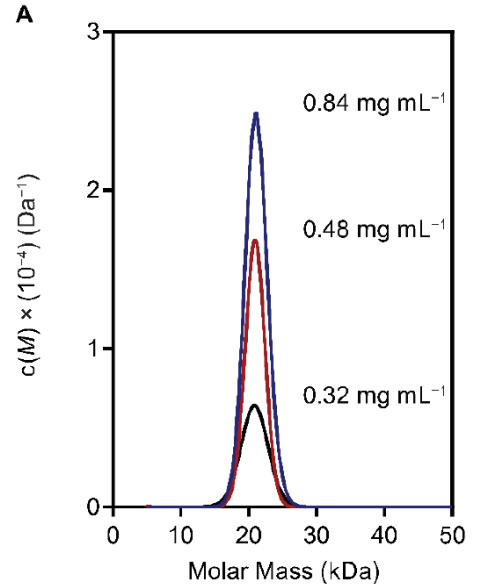

Sedimentation velocimetry reveals a single peak as a function of concentration – monomeric protein in solution

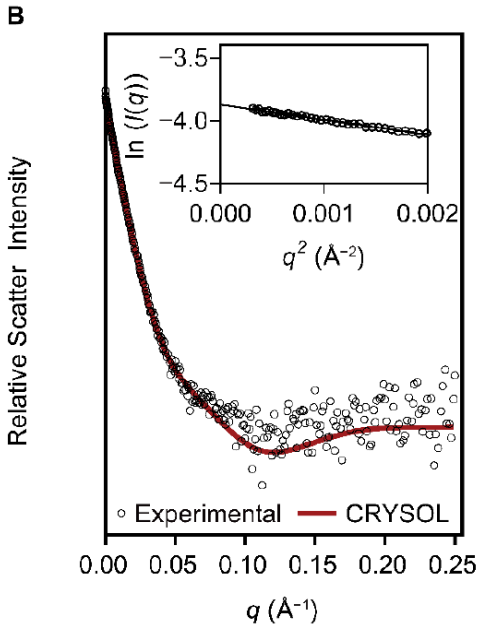

Comparison of calculated scattering pattern from single crystal structure (CRYSOL) reveals solution structure is the same

Love *et al. Viruses* 2021, 13, 1101

ANSTO

Protein-Drug Interactions in Solution

Plasminogen (Plg) exists in a closed conformation but must open up to be activated to plasmin (Plm) that breaks up blood clots, severe hemorrhages are managed with Plm inhibitors.

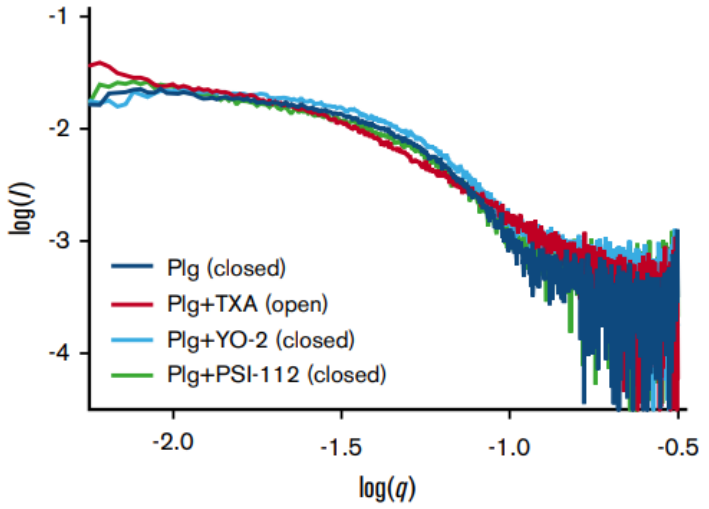

Sample	R_g (Å)	D_{max} (Å)
Plg (closed)	35.2 ± 0.5	115.3
Plg +TXA (open)	44.0 ± 0.4	174.6
Plg + YO-2	34.9 ± 0.7	115.0
Plg+ PSI-112	34.8 ± 0.7	123.4

Plm inhibitor TXA changes the solution structure of Plg, opening it up

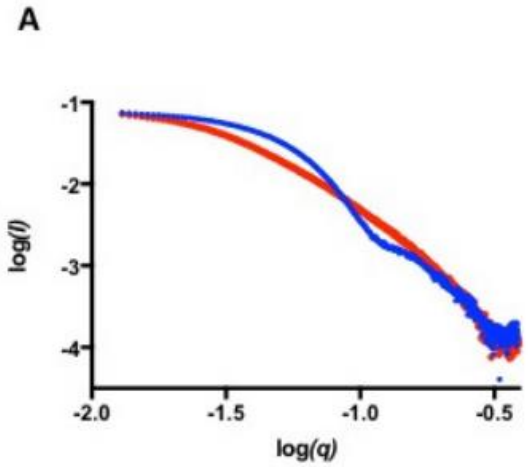

Bead modelling (DAMMIN, ATSAS) of the scattering from the open (red/C) and closed (blue/B) forms of the proteins overlays well with their single crystal structures

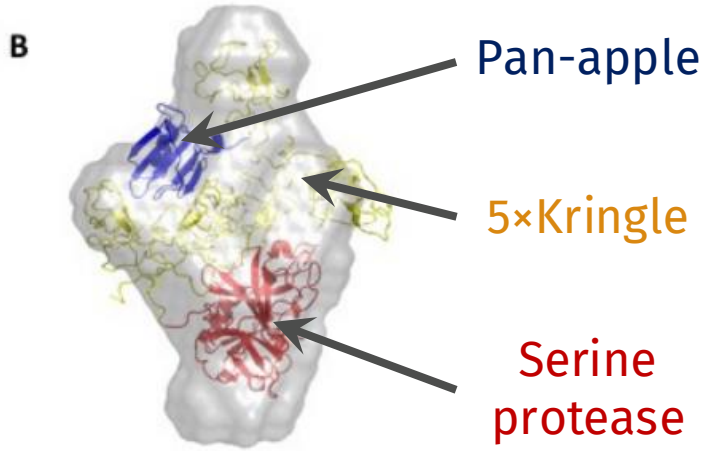

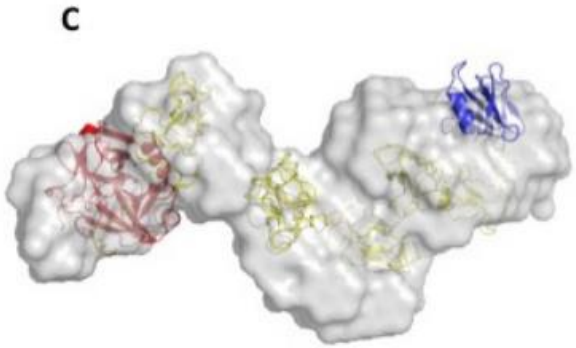

Law *et al. Blood Adv.* 2017, 1 (12), 766-771

ANSTO

Intrinsically Disordered Proteins

Low density lipoprotein type A module (LDLa) with linker domains from the GPCRs RXFP1 and RXFP2 adopt distinct conformational ensembles

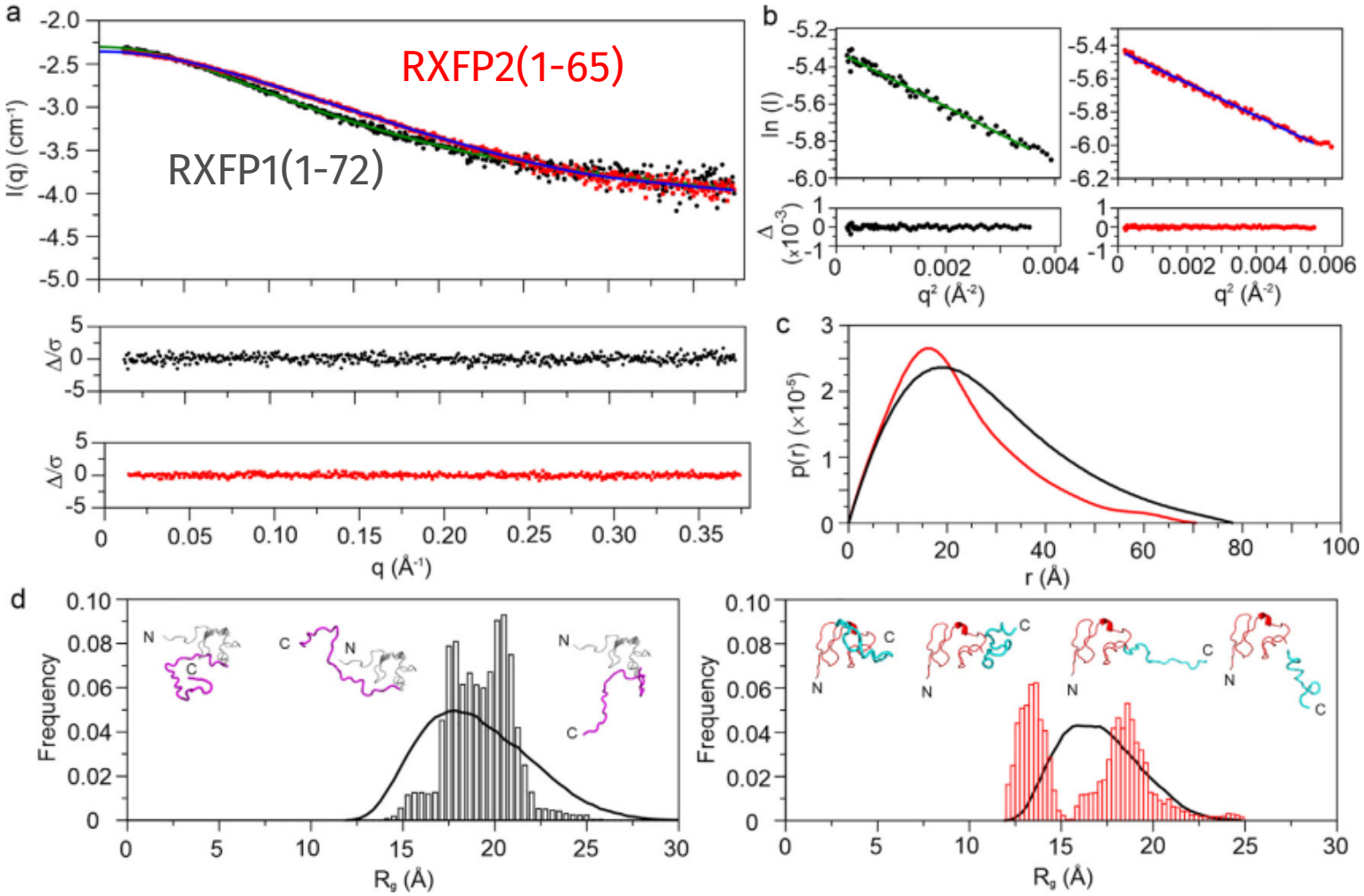

The GPCRs have different radii of gyration: RXFP1 = 21.06 ± 0.19 Å
RXFP2 = 15.98 ± 0.14 Å

The Ensemble Optimisation Method (EOM) was used to generate a pool of different conformations of the intrinsically disordered regions

RXFP1 – one main population, linker folds back
RXFP2 – two populations, linker extends in larger one, protein more globular in smaller one

Sethi *et al. J. Mol. Biol.* 2021, 433, 167217

ANSTO

Colloidal Systems

Typical Data Content – Mesophases

Lamellar (L_α)

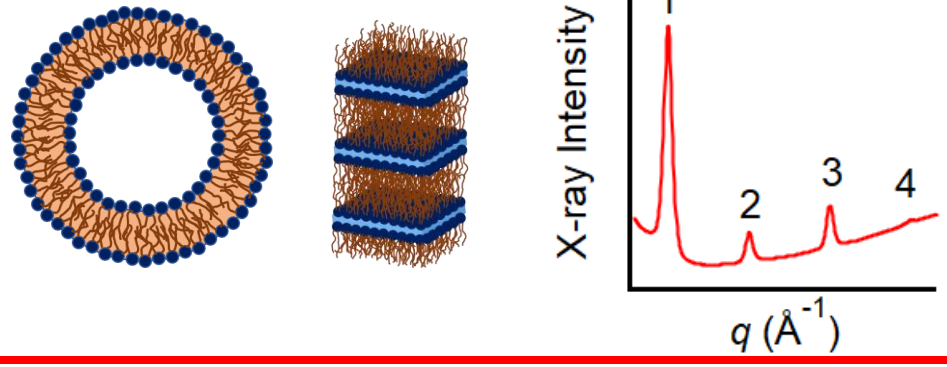

Inverse Micellar Cubic (I_2) and Disordered Micellar (L_2)

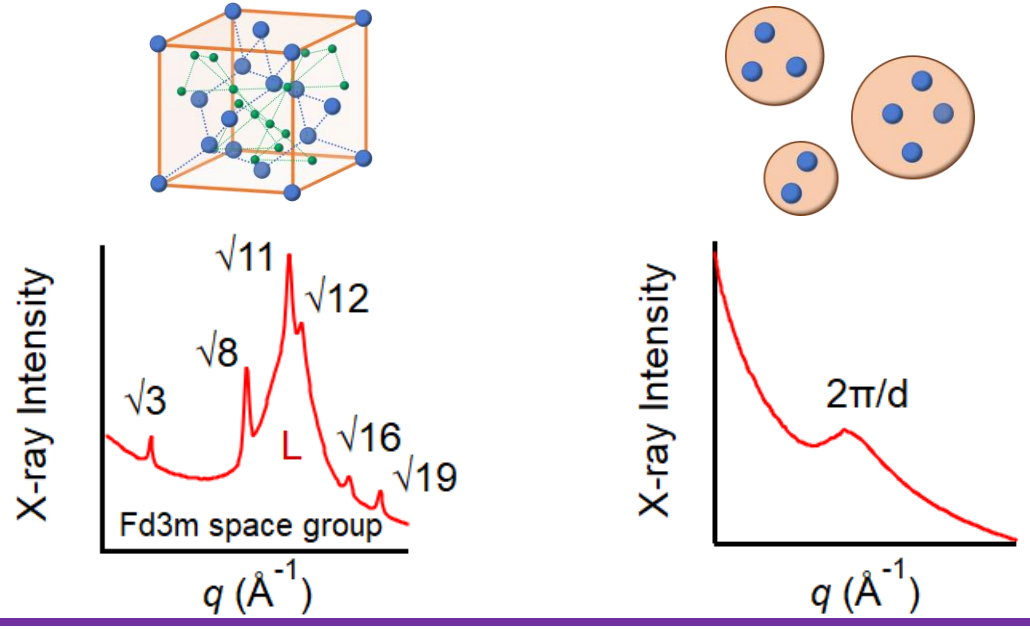

Inverse Bicontinuous Cubic (V_2)

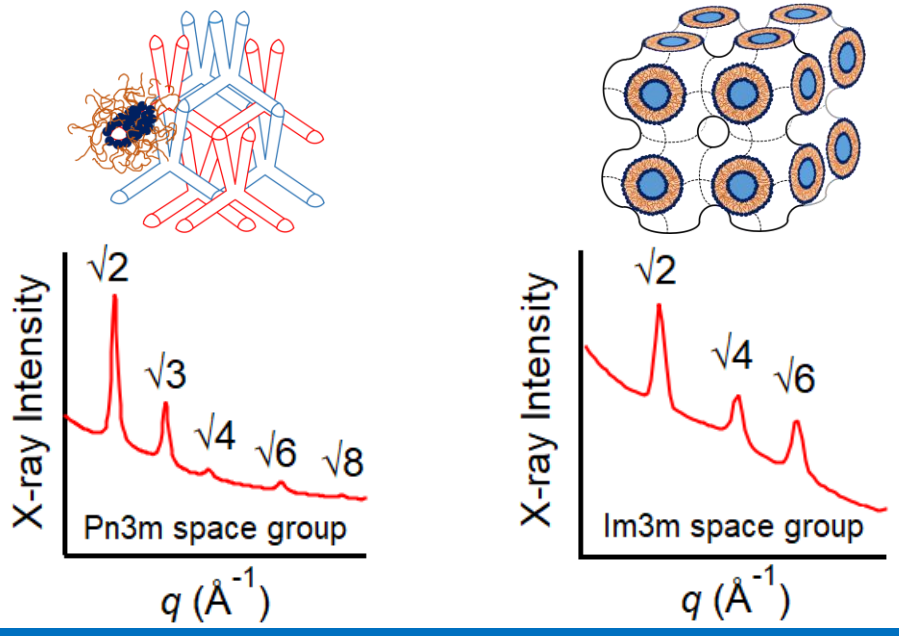

Inverse Hexagonal (H_2)

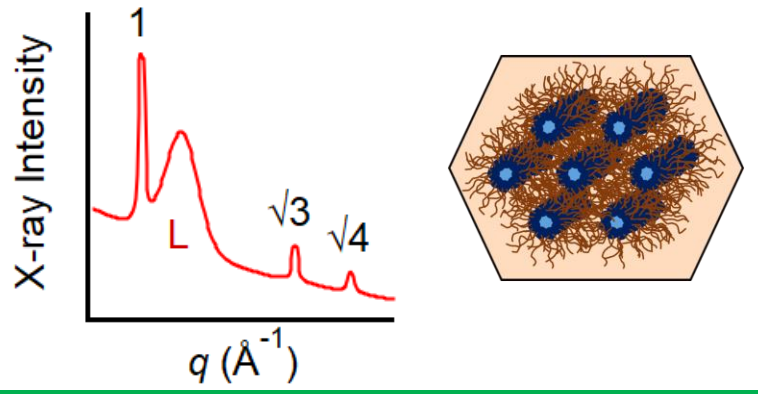

Time-resolved SAXS

Rearrangement of lipid mesophases in response to rapid change in pH upon mixing with acidic buffer

Lamallar to hexagonal to bicontinuous cubic transition

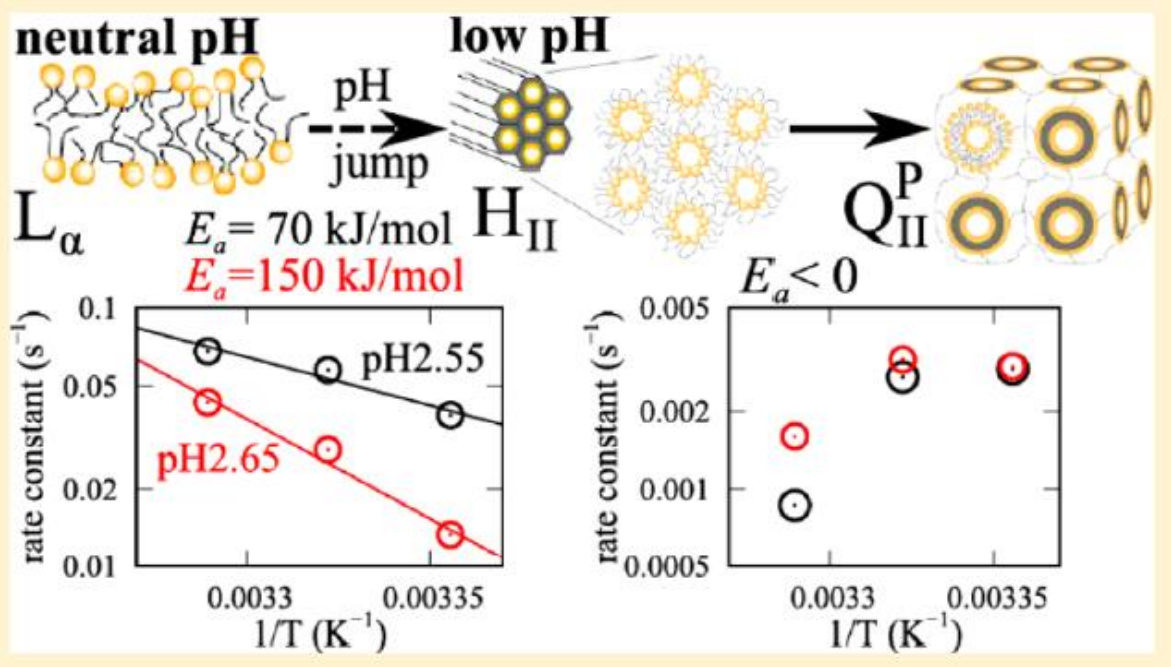

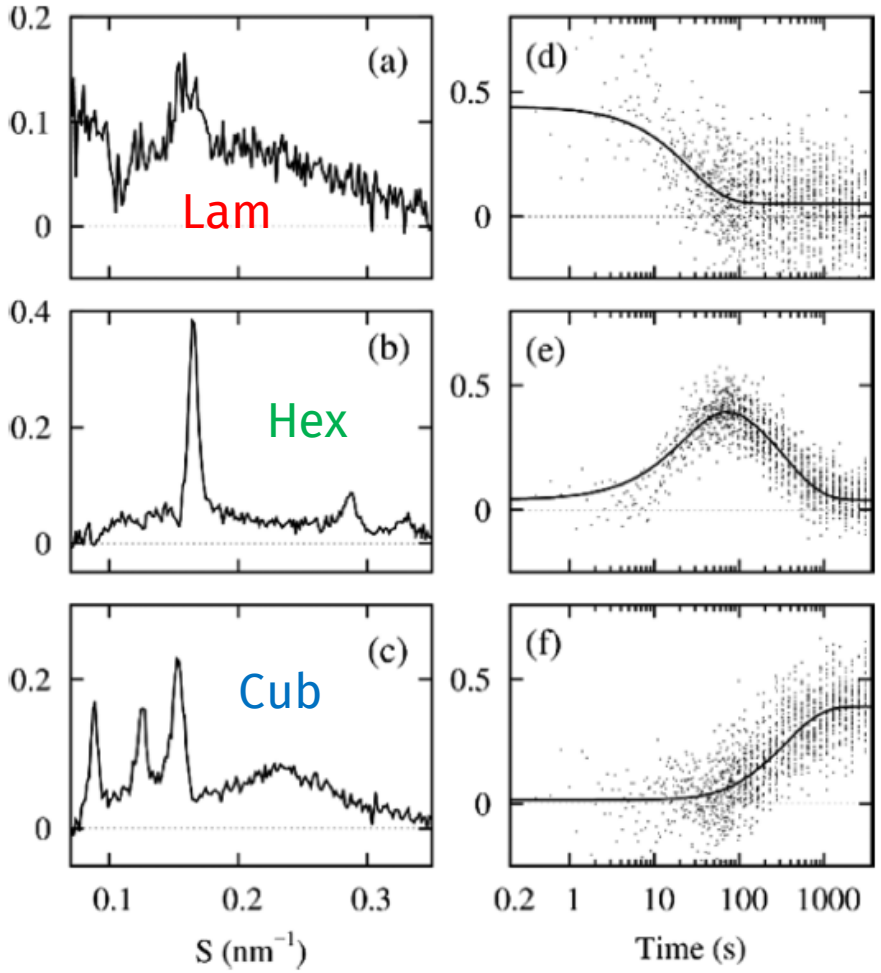

Allows access to rapid process kinetics
(200 ms – 9 s exposures)

Oka *et al. Langmuir* 2017, 33, 12487-12496

ANSTO

Typical Data Content – Particle Structure

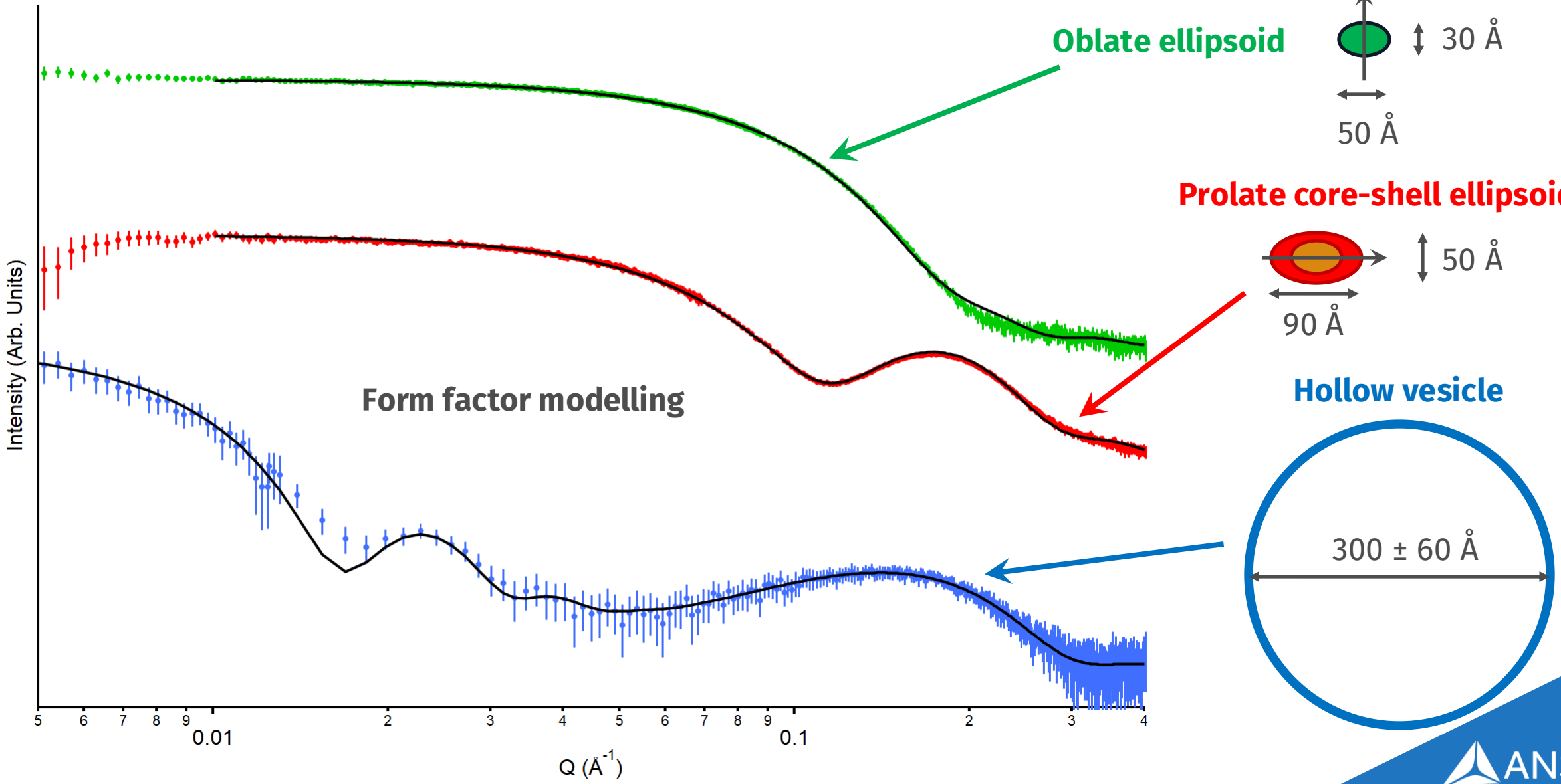

Growth of Nanoparticles in Solution

Growth of gold nanoparticles in solution by reduction of gold(III) acid by hydroquinone, the final geometry of the particles is rod-like

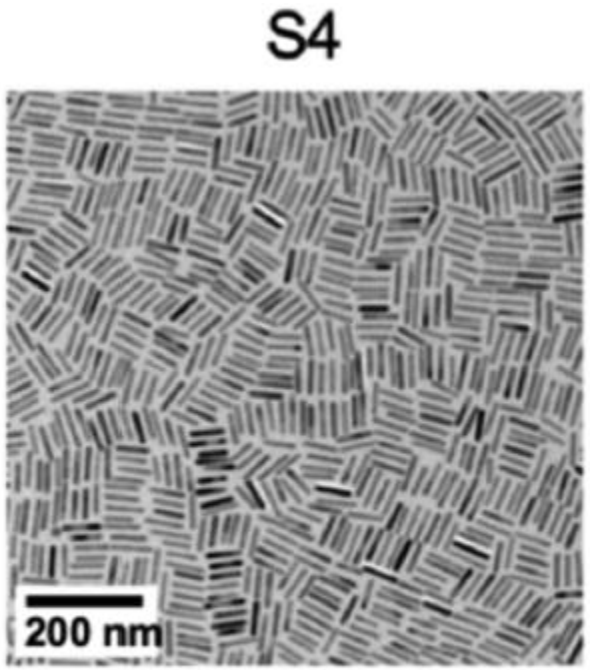

L = 54.0 nm ± 2.9 nm
W = 9.7 nm ± 0.4 nm

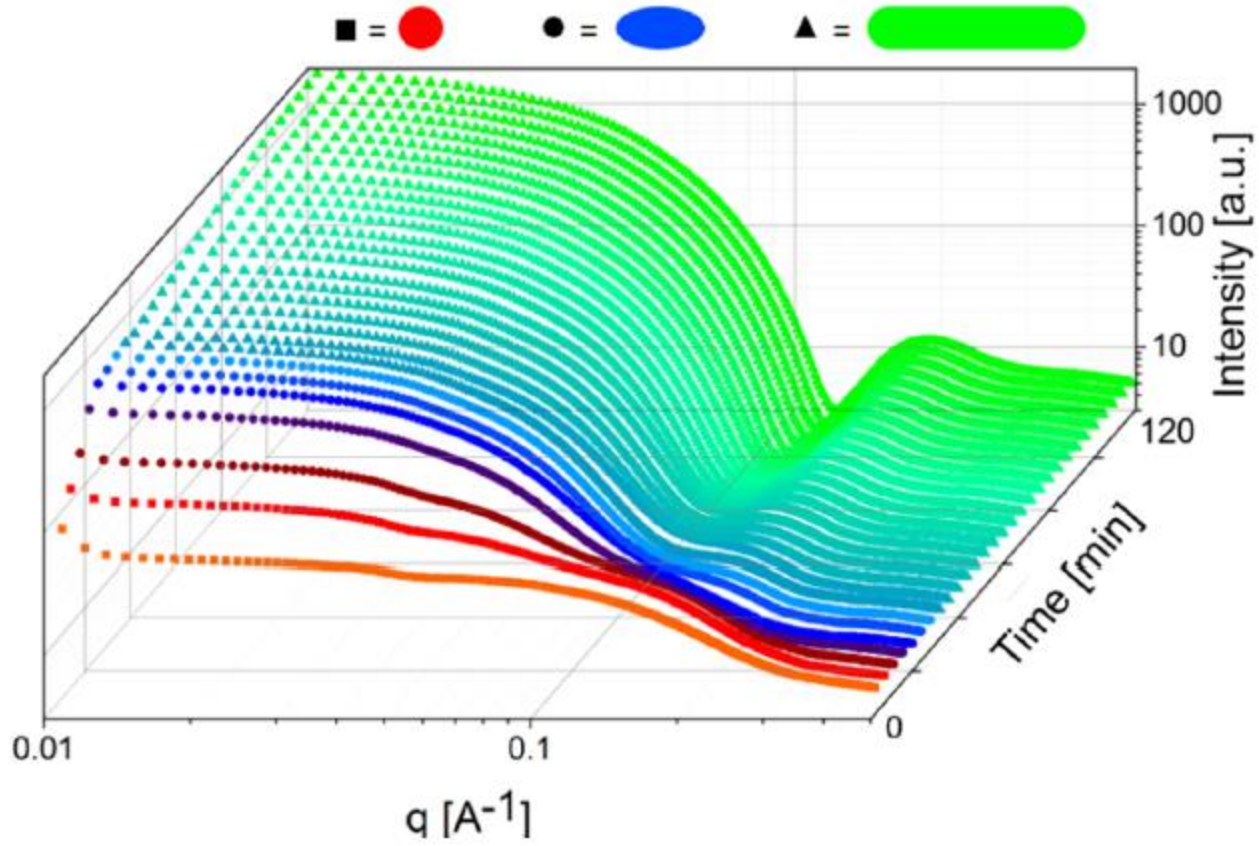

Time-resolved SAXS showed the transition from spherical to ellipsoidal to rod-like (cylindrical) particles during particle growth

Seibt *et al. J. Phys. Chem. C.* 2021, 125, 19947-19960

ANSTO

Grazing Incidence Scattering & Thin Films

ANSTO

Grazing Incidence Scattering

Very low incidence angles
(often <1°)
Surface-sensitive technique

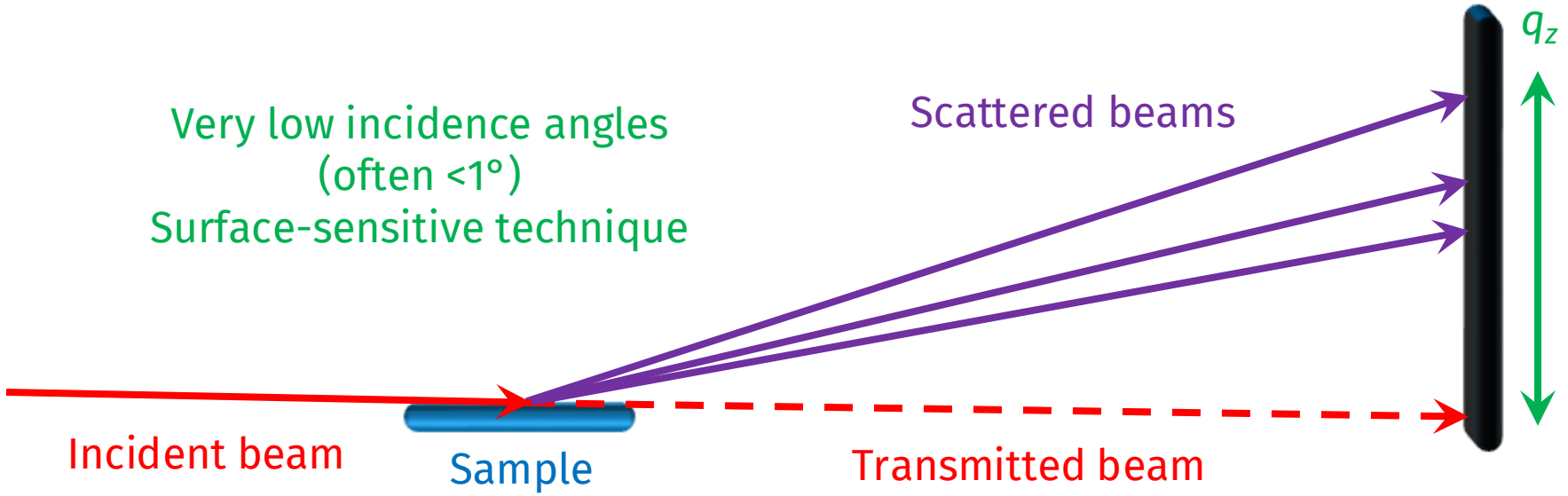

2D area detector

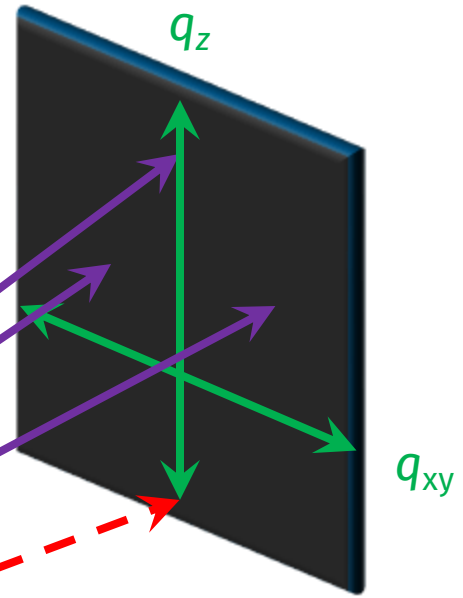

Provides information about scattering
out of the plane of the sample (q_z)
and in the plane of the sample (q_{xy})

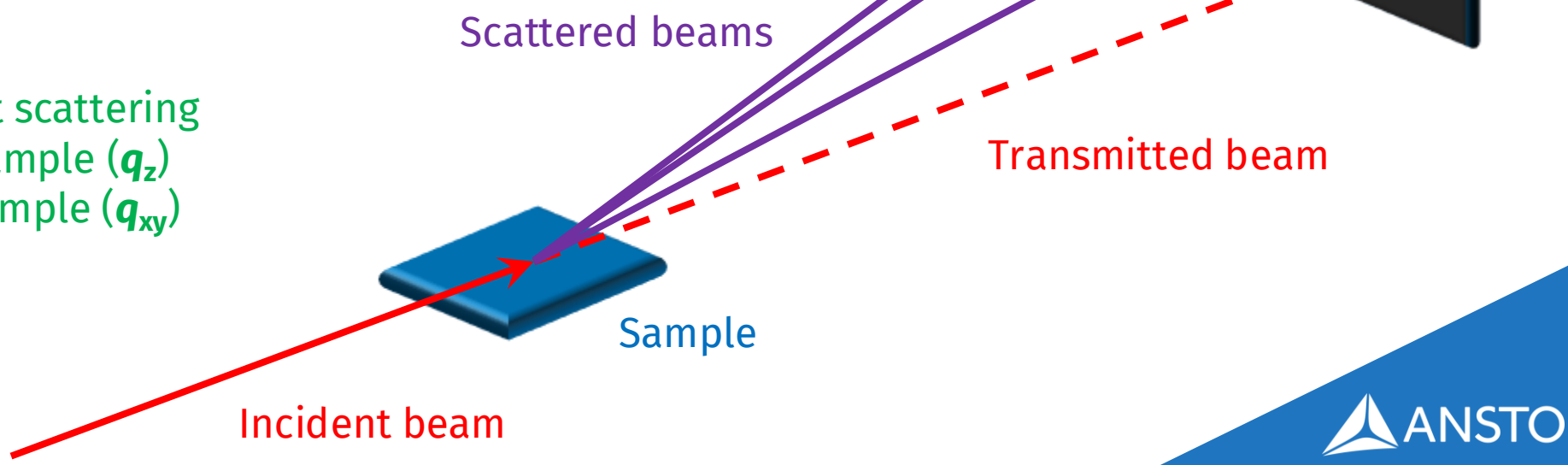

ANSTO

Surface Versus Bulk Sensitivity

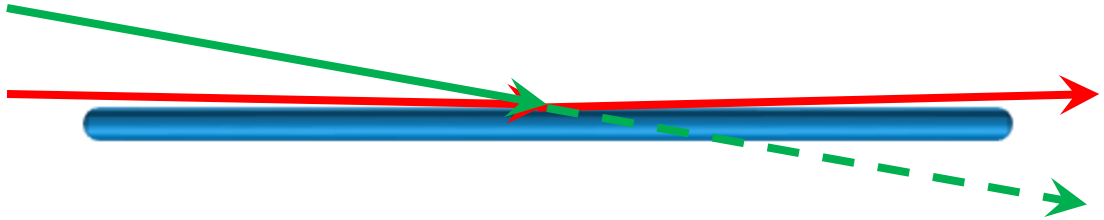

Beam below critical incidence angle is totally reflected

Beam above critical incidence angle is transmitted/absorbed

Penetration depth is X-ray energy dependent

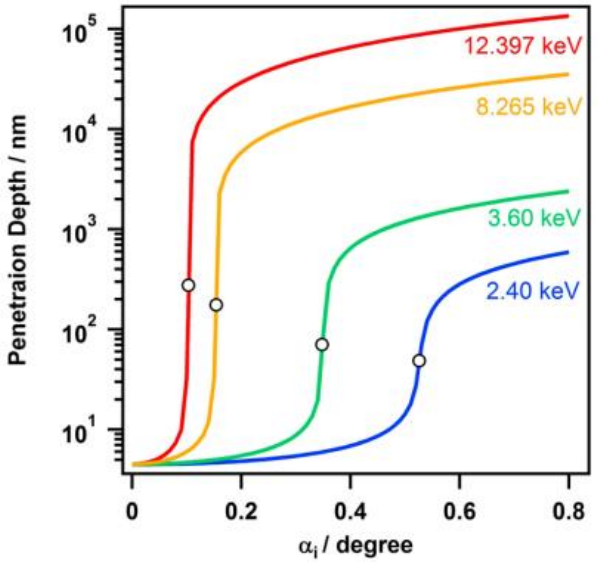

Penetration depth is material dependent

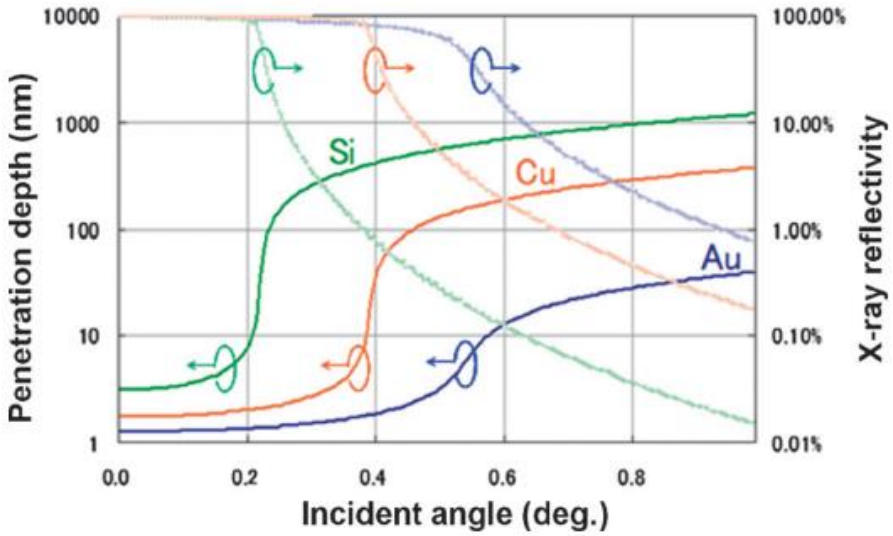

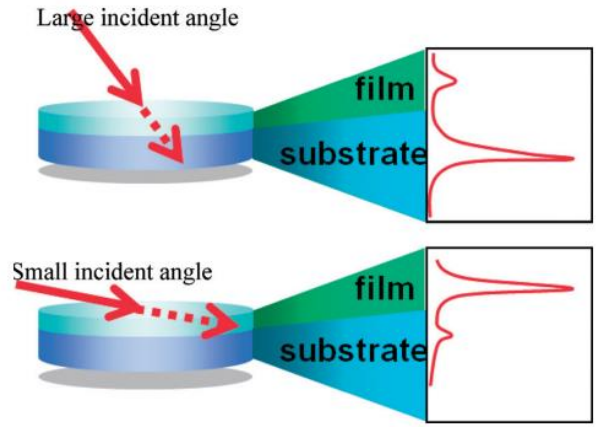

Saito *et al. Macromolecules* 2015, *48*, 8190-8196.

Kobayashi S. *Rigaku J.* Winter 2010, *26* (1) 03-11.

ANSTO

Thin Film Photovoltaics

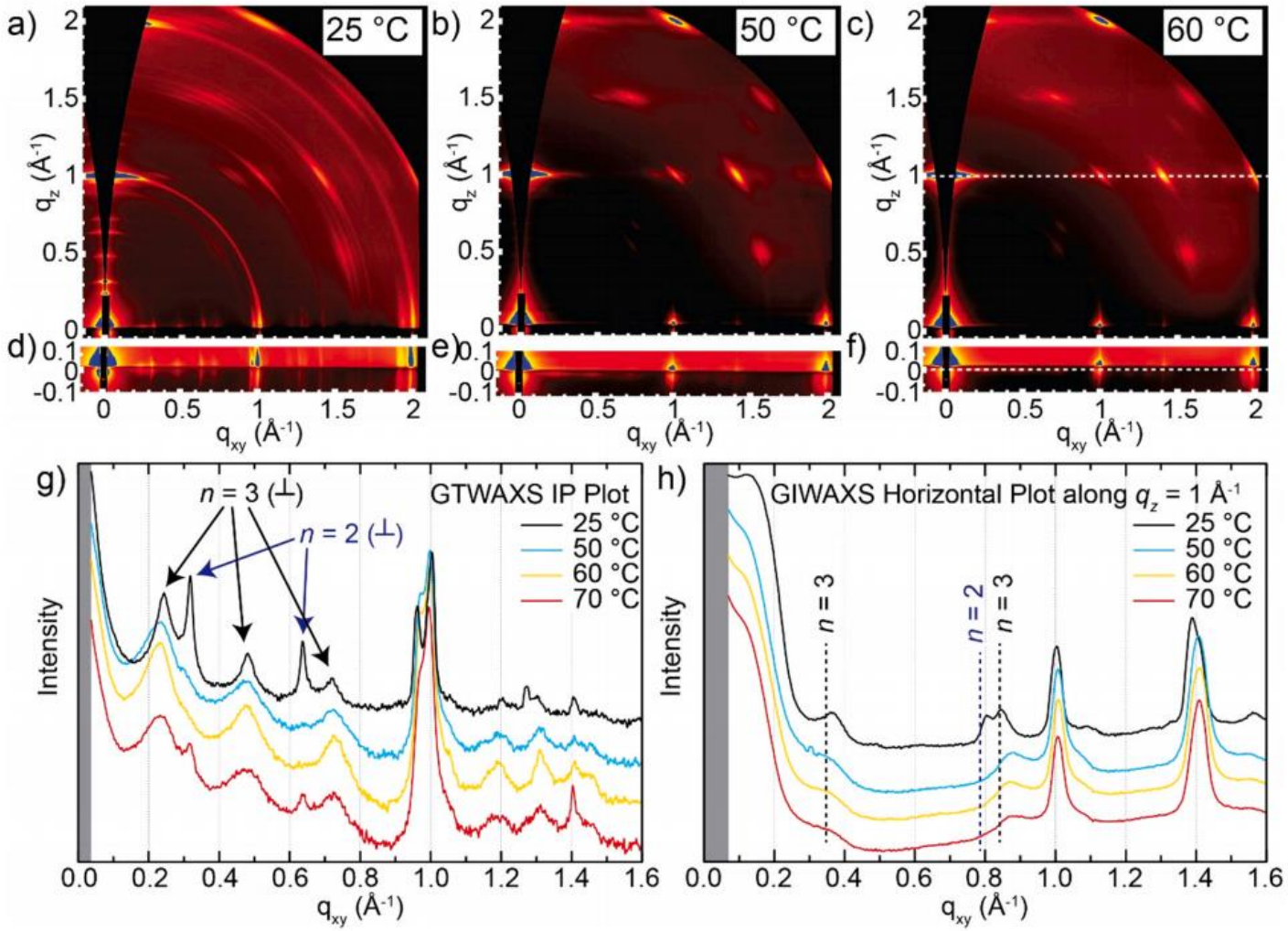

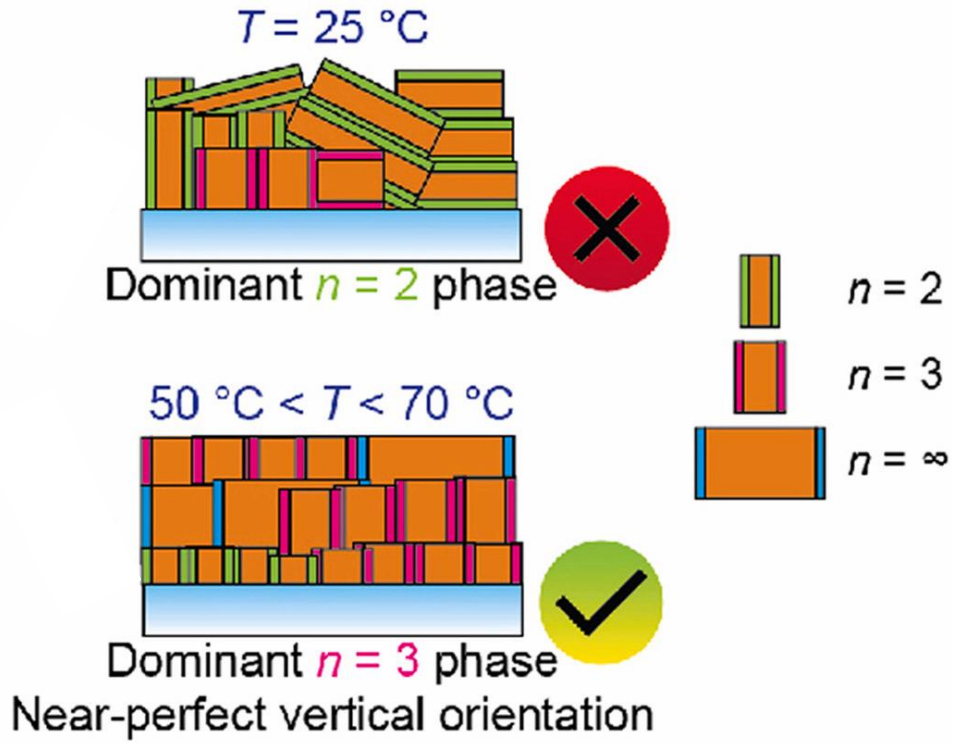

Tan *et al. Nano Energy* 2021, 83, 105818

Influence of blade coating temperature on structure of perovskite thin films

ANSTO

Solid State SAXS

ANSTO

Scattering from Collagen in Leather

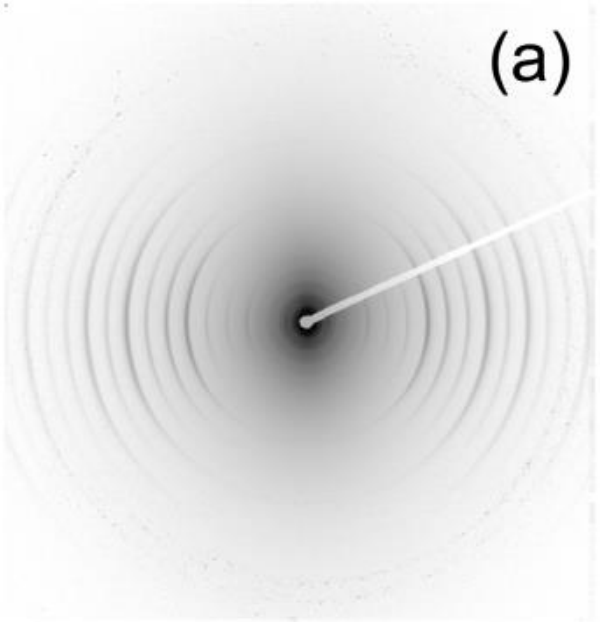

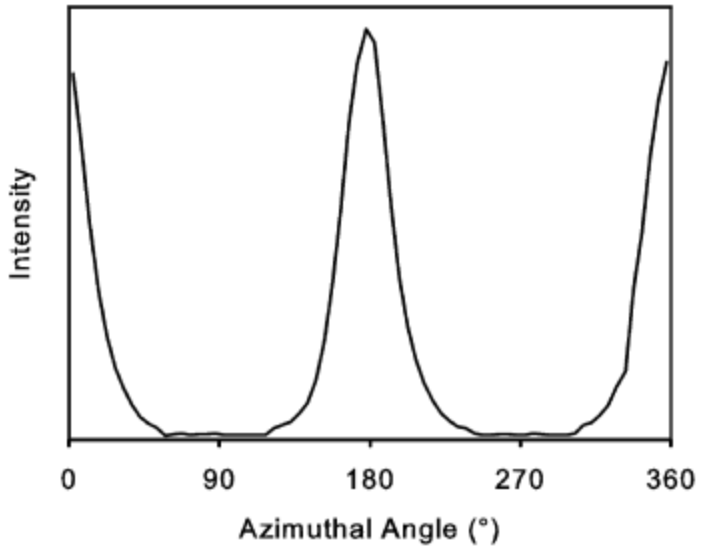

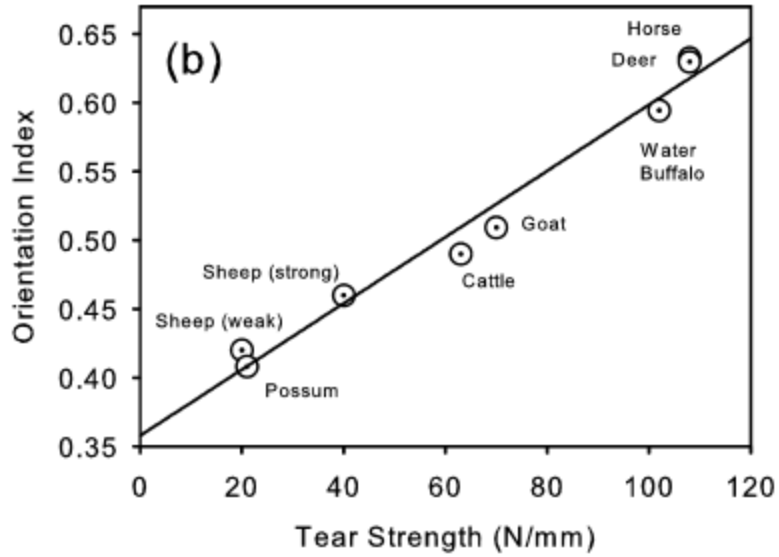

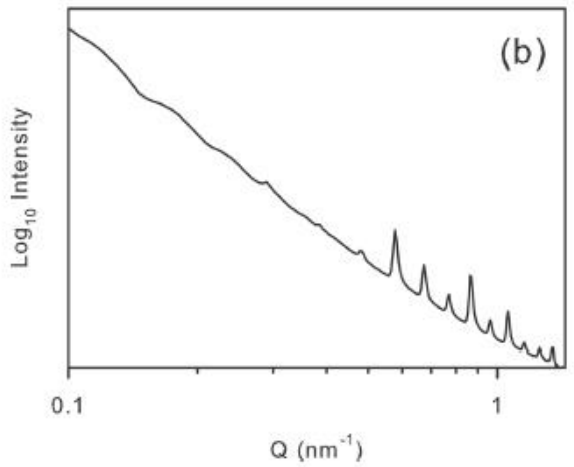

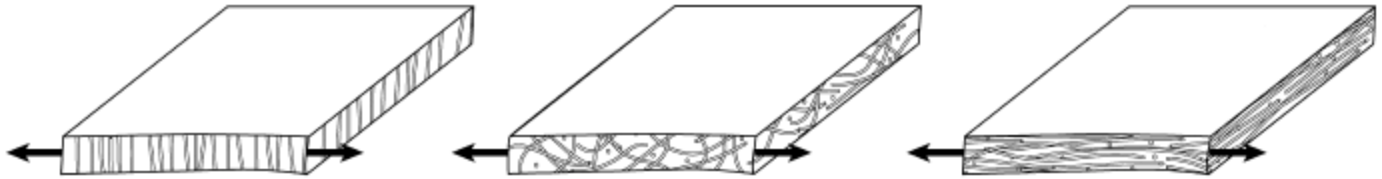

Collagen fibrils have a diffraction signal in the small angle region

The orientation index can be quantified from the position of the diffraction peaks and correlated with tear strength in leather

Sizeland *et al. J. Agric. Food Chem.* 2013, 61, 887-892

ANSTO

Scattering from Carbon Fibres

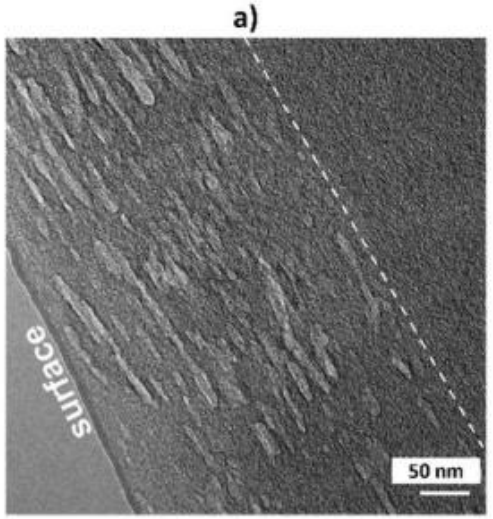

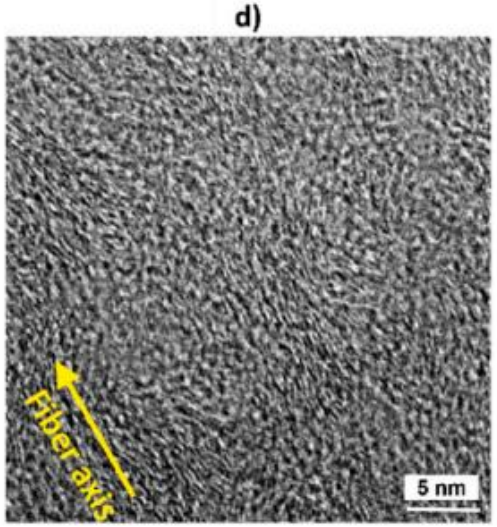

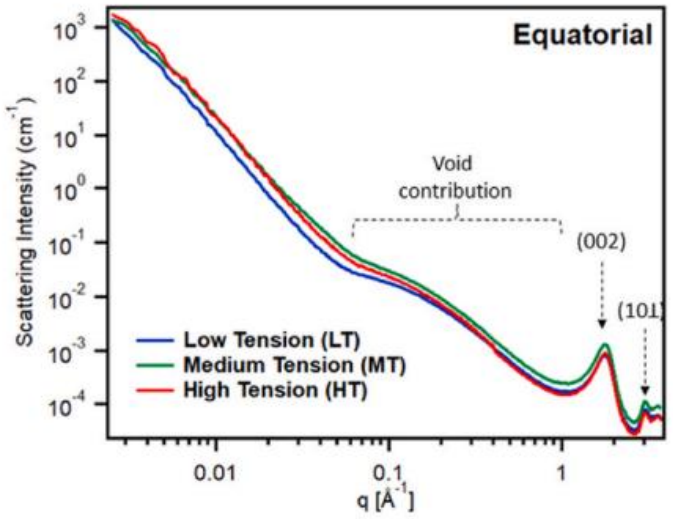

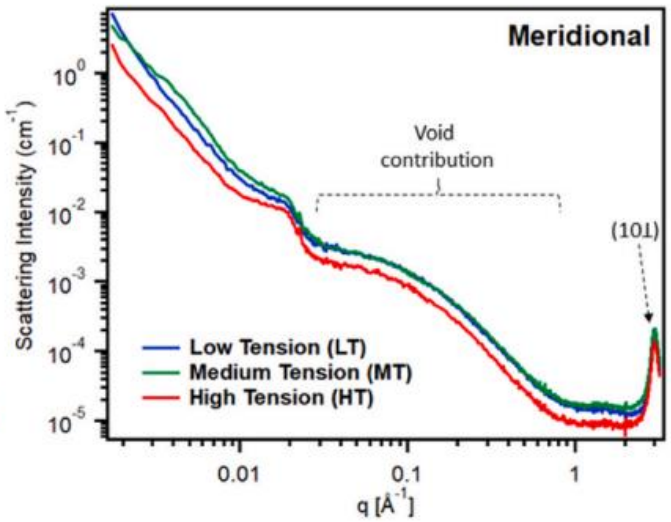

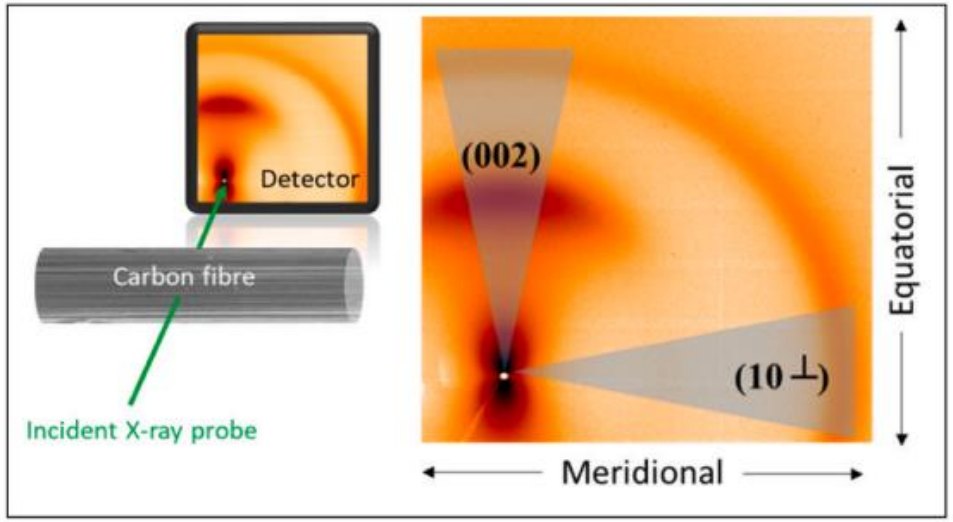

Orientation of voids and crystallites in carbon fibres yields highly oriented scattering profiles that can be characterised as a function of tension applied to the fibres

Xu *et al.*, *Carbon* 2023, 29, 117982

ANSTO

Myelin Orientation in Brain Sections

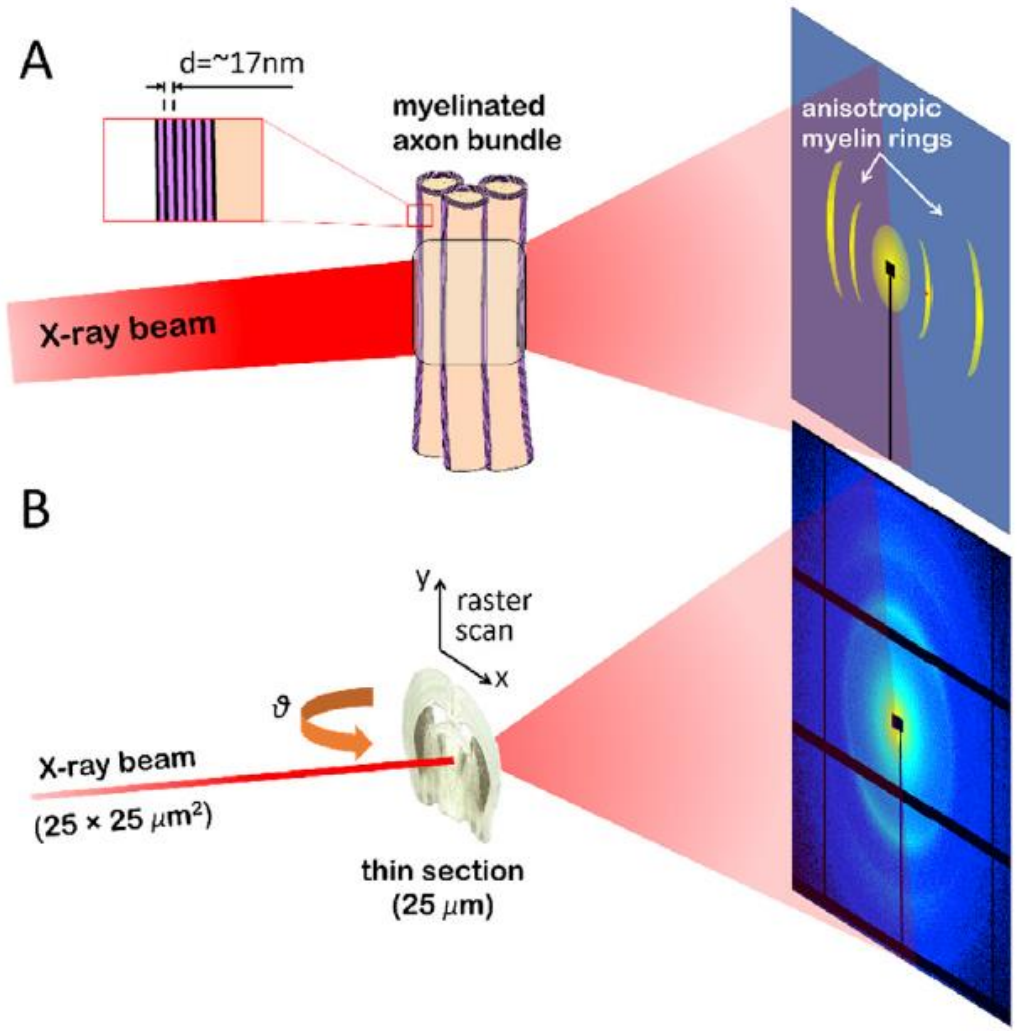

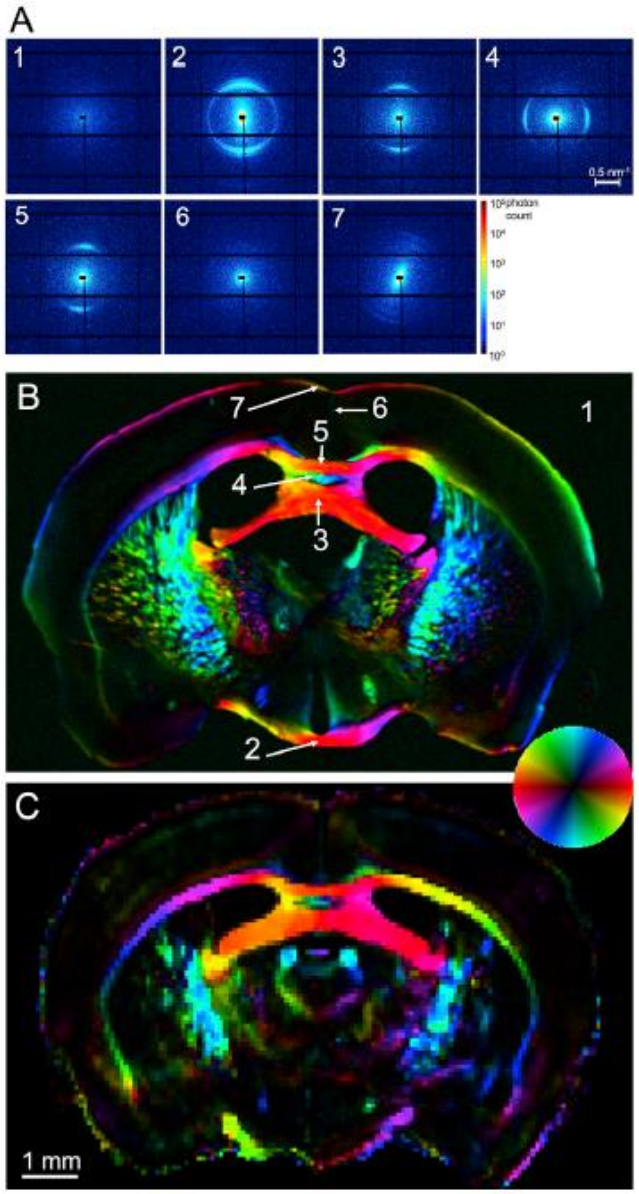

With a small bright synchrotron X-ray beam you can use scanning SAXS to measure the orientation of biological fibrils (myelin) in thin sections (Right Image B) for comparison with MRI scans (Right Image C)

Giorgiadis *et al.*, *NeuroImage* 2020, 204, 116214

ANSTO

Questions

(Over to you)